Portland State University

PDXScholar

Civil and Environmental Engineering Faculty Publications and Presentations

Civil and Environmental Engineering

9-7-2022

Warming of the Willamette River, 1850–Present: The Effects of Climate Change and Direct Human Interventions

Stefan Talke
California Polytechnic State University

David Jay
Portland State University, djay@pdx.edu

Heida Diefenderfer
Pacific Northwest National Laboratory

Follow this and additional works at: https://pdxscholar.library.pdx.edu/cengin_fac

Part of the Civil and Environmental Engineering Commons, Environmental Studies Commons, and the Water Resource Management Commons

Let us know how access to this document benefits you.

Citation Details

Talke, S.A., Jay, D.A., & Diefenderfer, H. (2023 submitted). Warming of the Willamette River, 1850–present: the effects of climate change and direct human interventions. submitted to Hydrology and Earth System Science, August 2022. EGUsphere [preprint], https://doi.org/10.5194/egusphere-2022-793

This Pre-Print is brought to you for free and open access. It has been accepted for inclusion in Civil and Environmental Engineering Faculty Publications and Presentations by an authorized administrator of PDXScholar. Please contact us if we can make this document more accessible: pdxscholar@pdx.edu.

https://doi.org/10.5194/egusphere-2022-793
Preprint. Discussion started: 7 September 2022
© Author(s) 2022. CC BY 4.0 License.

Warming of the Willamette River, 1850–present: the effects of climate change and direct human interventions

Stefan A.Talke[1], David A.Jay[2], Heida L. Diefenderfer[3,4]

[1]Civil and Environmental Engineering, California Polytechnic State University, San Luis Obispo, California

[2]Civil and Environmental Engineering, Portland State University, Portland, Oregon

[3]Coastal Sciences Division, Pacific Northwest National Laboratory, Sequim, Washington

[4]School of Environmental and Forest Sciences, University of Washington, Seattle, Washington

Correspondence to: Stefan A. Talke (stalke@calpoly.edu)

Keywords: Water Temperature, Climate Change, River regulation, Anthropogenic Effects

Key Points

- A statistical model based on archival records back to the 1850s shows that average water temperature has increased by 1.1 °C/century since the mid-19th century
- The largest increases in water temperature occur January–February (1.3 °C/century) and the smallest in May-June (~ 0.8 °C/century)
- The number of warm water days above 20 °C has increased by ~3 weeks, matched by a similar decrease in the number of days below 4 °C
- Approximately 30% of increased water temperature is attributable to system changes, and 70% to warming air temperature (climate change)

https://doi.org/10.5194/egusphere-2022-793
Preprint. Discussion started: 7 September 2022
© Author(s) 2022. CC BY 4.0 License.

Abstract

Using archival research methods, we found and combined data from multiple sources to produce a unique, 140 year record of daily water temperature (T_w) in the lower Willamette River, Oregon (1881– 1890, 1941– present). Additional daily weather and river flow records from the 1850s onwards are used to develop and validate a statistical regression model of T_w for 1850– 2020. The model simulates the time-lagged response of T_w to air temperature and river flow, and is calibrated for three distinct time periods: the late 19th, mid 20th, and early 21st centuries. Results show that T_w has trended upwards at ~1.1 °C /century since the mid-19th century, with the largest shift in January/February (1.3 °C /century) and the smallest in May/June (~ 0.8 °C /century). The duration that the river exceeds the ecologically important threshold of 20 °C has increased by ~20 days since the 1800s, to ~60 d yr^{-1}. Moreover, cold water days below 2 °C have virtually disappeared, and the river no longer freezes. Since ~1900, changes are primarily correlated with increases in air temperature (T_w increase of 0.81 ±0.25 °C) but also occur due to increased reservoir capacity, altered land use and river morphology, and other anthropogenic changes (0.34 ±0.12 °C). Managed release of water influences T_w seasonally, with an average reduction of 0.27 °C and 0.56 °C estimated for August and September. System changes have decreased daily variability (σ) by 0.44 °C, increased thermal memory, and reduced interannual variability. These system changes fundamentally alter the response of T_w to climate change, posing additional stressors on fauna.

Short Summary

This manuscript uses archival measurements and a statistical model to show that water temperatures in the Willamette River have trended upwards since 1850, with the largest increase occurring in winter and the smallest in late spring. Approximately 30% of the increase is attributable to system changes, and 70% to warming air temperature (climate change). The number of warm water days has significantly increased, and near freezing conditions, common historically, no longer occur.

1.0 Introduction

Water temperatures are rising in many temperate streams and rivers, in part due to climate change (e.g., Kaushal et al., 2010). Beyond a warming climate, many additional factors influence water temperature (T_w), including land-use patterns, water withdrawal and return flows, reservoir storage, and other types of water-resources management (e.g., Olden & Naiman, 2010; Bottom et al., 2011). Because water temperature influences ecological processes, water quality, oxygen levels, and fish habitat and survivability (e.g., Caissie, 2006, Bottom et al., 2011), defining long-term temperature trends and understanding their causes is vital. However, with few exceptions (e.g., Webb & Noblis, 2007; Pohle et al., 2019), few T_w records from the late 19th or early 20th century have been evaluated, particularly in North America (Kaushal et al., 2010). The limited availability of earlier records inhibits the ability to discern secular trends, evaluate causes, and assess impact. There is, therefore, a need to digitize and analyze archival water temperature records, such as those collected daily by the US Signal Service in the 1880s at 20+ coastal and river stations (see the Monthly Weather Review series of publications, volume 9 to 18).

https://doi.org/10.5194/egusphere-2022-793
Preprint. Discussion started: 7 September 2022
© Author(s) 2022. CC BY 4.0 License.

In the Pacific Northwest, T_w controls the long-term viability of salmon and other endangered species (Mantua, 2010; Bottom et al., 2011, Isaak et al., 2012, Caldwell et al., 2013). Above a threshold of 18–21 °C, various species of salmon, steelhead, and trout are stressed and become more susceptible to disease (OR DEQ, 2006, Mantua, 2010). As a result, regulations require that the seven day average of the daily maximum temperature should not exceed 20 °C, with a lower threshold set for rearing and spawning streams (e.g., OR-DEQ, 2006). An allowance of 0.3 °C is permitted for the sum of all anthropogenic point sources such as wastewater discharge, and non-point sources such as loss of shading or heating in reservoirs. Hence, the Willamette River in Portland, Oregon (Figure 1) is considered an impaired water body and out of regulatory compliance for T_w above 20.3 °C (OR DEQ, 2006).

Accurately assessing and disentangling anthropogenic and climate change influences is challenging because of the large number of alterations and anthropogenic uses (e.g., diversions and discharges), and feedbacks between different factors. Compared to its natural state, the Willamette River is more channelized, deeper, and reduced in length (particularly in upstream reaches; e.g., Sedell and Froggatt, 1984; Benner and Sedell, 1997; Gregory et al., 2002a). The construction of large storage reservoirs (Payne, 2002) has altered flow patterns and heating patterns within the basin, and several hydroelectric projects increase T_w (OR DEQ, 2006). Logging within the watershed reduces shading and also increases T_w (Johnson & Jones, 2000). Nonetheless, summertime peak T_w values at reservoir sites likely decreased after dam construction, because of increased water depths; at the same time, autumn temperatures have increased (e.g., Angiletta et al., 2008; Rounds, 2010). Below the storage reservoirs, channelization of the Willamette, deforestation of the riparian corridor (decreased shading) (Gregory et al. 1991, Wallick et al. 2022), water diversions, and storage for agriculture have also likely shifted T_w (Berger et al., 2004). Because of a lack of in-situ data from pre-reservoir conditions, the cumulative effect of anthropogenic influence since European settlement is currently unknown (OR DEQ, 2006).

Hydrological and land-use changes in the Willamette Basin have occurred within a background of a warming climate and hotter extremes. The summers of 2009, 2015, and 2021 were dry and hot in the Pacific Northwest, with conditions consistent with the future climatology predicted by climate models (e.g., Mote and Salathé, 2010, Bumbaco et al., 2013). In 2015, snowpack was extremely low, leading to record low streamflow in many rivers (Mote et al., 2016). The combination of hot, dry weather and low river discharge produced elevated water temperatures, adversely affecting salmon populations (Crozier et al., 2020). However, despite record heat waves during the summer of 2021 (Portland reached a record air temperature of 46.7 °C, about 5 °C above the previous all-time high), water temperatures in the Willamette River, a major tributary of the Columbia River, did not reach the peak of 2015.

Anomalously hot years are useful for understanding processes that control T_W, and characterizing natural variability in the context of climate change. How anomalous were water temperatures in coastal rivers in the Pacific Northwest during 2009, 2015 and 2021, and to what extent has climate change influenced extremes? How much have water temperatures changed from natural, background conditions? The dearth of long-term data complicates assessment of patterns and trends, since weather patterns such as El Nino/La Nina and the Pacific Decadal Oscillation influence interannual and decadal variability in T_W (Peterson & Kitchel, 2001). Also, the construction of reservoirs, deforestation of the riparian corridor, irrigation diversions, and other land-use changes are known to influence flow hydrographs and T_w in other basins (e.g., Olden & Naimen,

https://doi.org/10.5194/egusphere-2022-793
Preprint. Discussion started: 7 September 2022
© Author(s) 2022. CC BY 4.0 License.

2010). Because chronic and acute anthropogenic factors change over time, they may mask or accentuate climate-induced variability and trends in degradation or recovery (NASEM 2022).

To investigate the secular changes in water temperatures caused by climate change and local anthropogenic influence, we construct a unique, instrument based T_w data set on the lower Willamette River (OR) that extends back to 1881, a time period with a cooler climate and unimpeded, natural flows. Water temperature records were found and digitized from various federal, state, and local archives, producing ~90 years of daily records stretching over a 140 year period. Seasonal patterns and long-term trends are assessed, and their relationship to local air temperatures are evaluated using a stochastic regression approach. Results show that extreme summertime water temperatures similar to 2009 and 2015 are found in the historical record (e.g., 1889 and 1941), and that water temperatures have frequently exceeded 20 °C during the summer, even in the 19th century. However, on secular time scales, average water temperature is rising during all times of the year, and the number of warm-water days is increasing. Therefore, temporal refugia during the time periods most conducive to coldwater species are becoming increasingly scarce.

2. Background and Methods

2.1 Setting

The Willamette River (Figure 1), with a mean annual discharge of 940 m^3/s (1971– 2020 period), drains approximately 29,700 square km of coastal Oregon (Figure 1; Branscomb et al., 2002). It is the 13th largest river in the contiguous United States by volume (Wallick et al. 2022), and its waters discharge into the larger Columbia River approximately 162km from the Pacific Ocean. The lower Willamette River, the focus of this study (Figure 1), is an approximately 43 km long region influenced by ocean tides during low-flow conditions and by backwater from the Columbia River, particularly during spring (Helaire et al., 2019). Because of its location near the mouth, the lower Willamette is influenced by and integrates climate changes and local anthropogenic changes occurring throughout the basin. Their net effect on T_w is explored in this manuscript; here, we first review the time history and magnitude of anthropogenic changes.

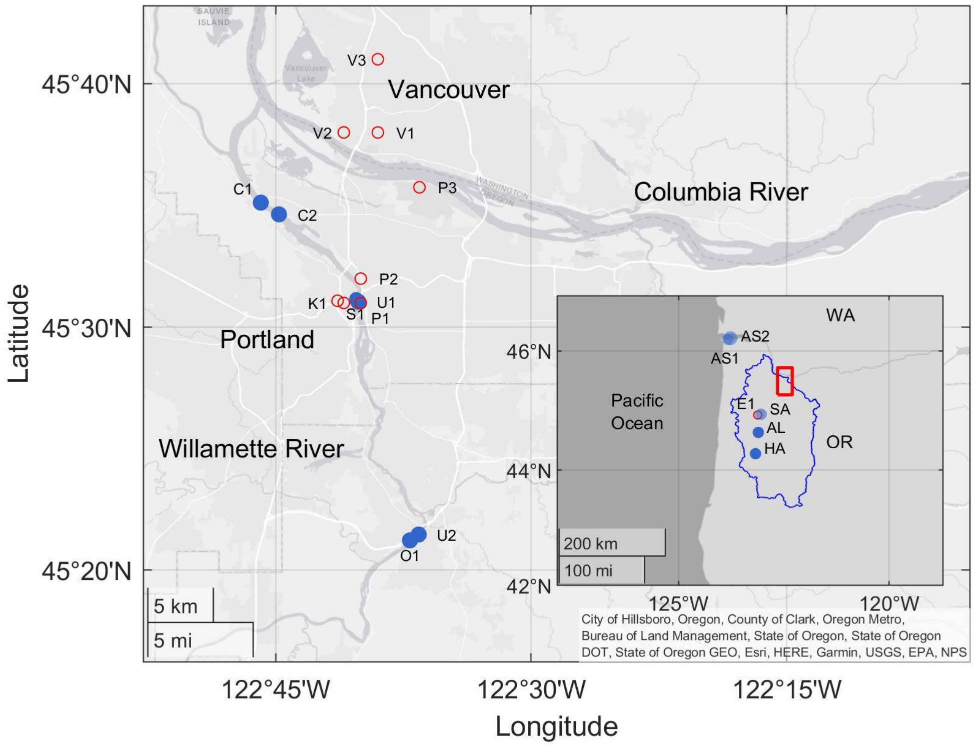

Figure 1: Site map with locations of T_w (blue, closed circles) and T_a (red, opencircles) measurements. The red bounding box in the inset denotes the Portland/Vancouver Metropolitan Area depicted in the larger figure. The Willamette River watershed boundaries are denoted in blue. OR = Oregon, WA = Washington. Abbreviations and period of record of the measurements are provided in Table 1.

The Willamette Basin has a temperate climate marked by overcast conditions from October–May, and predominately sunny, dry conditions from approximately mid-June to mid-September. Average annual precipitation on the valley floor is ~100– 130 cm/yr., with up to 500 cm occurring in the Cascade Mountains (Baker et al., 2002). Rainfall occurs primarily between October and May, with the wettest period occurring between November and January. At Portland, the largest discharge typically occurs during winter storms and peaks in the November– February period (Figure 2a). Historically, snow-melt driven flows contributed to elevated flows in the March–May time frame (Figure 2a). The combination of declining snowpack (e.g. Mote et al., 2018) and water management (e.g., Rounds, 2010) has reduced spring discharge. During summer, 60–80% of river water derives from high elevation regions above 1200m, either as direct snowmelt or as groundwater (Brooks et al., 2012). Late summer discharge has increased, however, because of the managed release of water. In the future, unimpeded wintertime discharges are expected to increase while summertime flows decrease (e.g., Chang & Jung, 2010).

© Author(s) 2022. CC BY 4.0 License.

The lower 300km of the Willamette River runs south-to-north through the Willamette Valley, which is now primarily agricultural. For thousands of years the Willamette Basin was inhabited by Native Americans, who influenced the watershed in many ways, including through controlled burns and small-scale fish dams (Boyd, 1999, Johannessen et al. 1971, Taylor, 1999). European settlement began in the early 1800s; Portland, founded in 1843, became the largest city in Oregon by 1860 (US Census, 1866). Shading has been reduced in its modern, channelized configuration compared to historical norms (Lee et al. 1995; OR-DEQ 2006). Land under irrigation was minor before 1910, and increased from ~13,500 hectares in 1945 to about 110,000 hectares by 1979 (Sedell & Froggatt, 1984). East side tributaries such as the Clackamas River (Willamette Rkm 40), the Mollalla River (Rkm 58) and the McKenzie River (Rkm 282) drain the mountainous Cascade Range, and flow primarily through steep forested regions. West-side tributaries such as the Tualatin River (Rkm 45) and the Long Tom River (Rkm 240) drain the lower, forested Coast Range and are slower moving (Lee et al., 1995). The Willamette splits into the Middle and Coast-fork at ~ Rkm 301; the headwaters of the Middle fork are approximately 486km from the confluence of the Willamette and the Columbia rivers.

The mainstem of the Willamette River has been extensively modified since the latter part of the 19^{th} century, first for navigation and agriculture, and later for flood control. Pre-European settlement, the river was maintained in a prairie or savannah-like condition by burning (Christy and Alverson 2011). After burning ceased (~ late 1700s), the river became fringed by a 3–7 km wide floodplain covered by a dense riparian forest (Thilenius 1968, Sedell & Froggatt, 1984). In the 1850s, approximately 97,500ha of the Willamette Valley was mapped by the Government Land Survey Office as riparian and wetland forest, and was dominated by tree species such as *Quercus garryana* (Oregon white oak), *Fraxinus latifolia* (Oregon ash), *Acer macrophyllum* (bigleaf maple), *Alnus rubra* (red alder), and *Populus trichocarpa* (black cottonwood) (Christy and Alverson 2011). The river planform was dynamic; the upper 200km typically contained 2– 5 shallow (1.5–3 m deep), braided channels that evolved each year due to the formation of gravel bars and driftwood barriers (Sedell & Froggatt, 1984; Gregory et al., 2002a; Wallick et al. 2022). Beginning in the 1870s, but particularly in the first half of the 20^{th} century, the river was reduced to a primarily single-thread stream, and shortened by nearly 20km (Sedell & Froggatt, 1984; Gregory et al., 2002a). Bank-stabilization measures began in the late 1800s and occurred most prominently during the mid-20^{th} century (1930s– 1960s); approximately 25% of Willamette River banks now have revetments, armoring, wing dikes, and other bank protection measures (Gregory et al., 2002b). Further, from 1870– 1950, approximately 65,000 "snags" (30– 60m long trees with a diameter of 0.5– 2m) were removed (>500 per km; Sedell & Froggatt, 1984). Peak snag removal occurred in the late 1800s/early 1900s (Sedell & Froggatt, 1984). These snags were often used to block-up side channels. As a result, off-channel areas such as alcoves and sloughs—often 2– 7 ^{o}C cooler than the mainstem—have decreased in extent by 70– 80% (Landers et al., 2002). Additionally, the forested area in the floodplain has decreased by 75-90% (Landers et al., 2002, Gregory et al. 2019). Dredging further altered the river, after its authorization in 1906. Between 1908– 1929, approximately 78,000 m^3 yr^{-1} of sediment were removed from the river above tidewater (Willingham, 1983), but much more extensive dredging has occurred in Portland Harbor. The depth of the river is currently ~ 12m in the lower ~20km of the Willamette, the focus area of our study (Figure 1). Depths gradually reduce to a centerline depth as shallow as 1.5– 2m around Rkm 280 (US Geological Survey (USGS), 2003).

https://doi.org/10.5194/egusphere-2022-793
Preprint. Discussion started: 7 September 2022
© Author(s) 2022. CC BY 4.0 License.

A total of 371 reservoirs and impoundments of various size have been built in the Willamette basin, with a combined capacity of more than 3.3 km^3 (Payne, 2002). Given a mean discharge of about 980 m^{3}s^{-1} (Naik and Jay, 2011), these reservoirs store ~10.6% of the annual average flow. The majority were built between 1950– 1980, with ~23 built pre-1950 and ~25 after 1980 (Payne, 2002). Approximately 45% are small storage reservoirs for irrigation (order 100,000 m^3 capacity); hydroelectric dams (~9%) and water supply reservoirs (6% of total) are typically of similar size (Payne, 2002). A total of 13 federal reservoirs for storage and flood control were built between 1941 and 1969 with a combined maximum storage capacity of 2.75 km^3 (Rounds, 2010); the largest are Detroit Dam (completed 1953, capacity 0.56 km^3), Lookout Point Dam (completed 1954, capacity 0.59 km^3) and Green Peter Dam (0.53 km^3 capacity, completed 1968; Payne, 2002; Rounds, 2010). The two federal reservoirs built in the 1940s were relatively small (combined capacity of 0.18 km^3) compared to modern capacity; therefore, we consider the period before 1953 to be pre-river flow regulation. An examination of hydrological records suggests that flood control exerted some influence in the 1954– 1964 period, reducing peak flows during the December 1964 flood considerably, and that the modern hydrological regime began ~1965– 1970 (Gregory et al., 2002c). In total, reservoirs have increased the surface area of water within the system by about 200 km^2, with the majority (80– 85%) occurring in the 13 federally operated water projects (Payne, 2002). A net increase of ~50 km^2 in water surface area is estimated for the Willamette Valley since 1851 (Gregory et al., 2002d), in part from water impoundments. By comparison, channelization between 1850 and 1995 only removed ~ 17 km^2 of water surface on the mainstem Willamette, from 76 to 59 km^2 (Gregory, 2002a). Combined with the loss of riparian corridor shading during the growing season (Gregory et al., 2002e; Rounds, 2007), the increased surface area in the basin means that heat input into the fluvial system—for the same meteorological conditions—has increased.

2.2 In-situ water temperature measurements

A number of measurements were obtained to assess changes to meteorological and fluvial conditions since the mid-19th century (Figure 1; Table 1 & Table 2), and approximately 30 years of archival records were digitized. From 1881– 1890, the US Signal Service (USSS) measured top- and bottom T_w at Portland at 11:00 (local time) every day. The successor to the USSS, the US Weather Bureau (USWB) measured T_w from 1941– 1961 between 6:30 am and 7:30 am daily (local standard time). We digitized and quality assured the previously unanalyzed USSS and USWB records, which were obtained from the National Centers for Environmental Information (NCEI). A spot-check of US Army Corps of Engineers records from Willamette Rkm 10.5 from 1941– 42 (Moore, 1968) showed a general consistency with USWB measurements, to within 1^o C. Measurements of T_w are available from the US Geological Survey (USGS) since 1961, with ~26 station years available in the Portland metropolitan area since 1971 (Table 1). Such federal records are supplemented by additional state and local records. Intermittent Grab-sample measurements of T_w are available from the State of Oregon Department of Water Quality, particularly during summer (1949, 1953– present; obtained from the City of Portland). Nearly continuous daily measurements of T_w at the Willamette Falls fish ladder from 1985– 2020 were obtained from the Oregon Department of Fish and Wildlife. Finally, a long, continuous record has been made available by the City of Portland at half-hourly increments from 1992– 1999 and 1997–

https://doi.org/10.5194/egusphere-2022-793
Preprint. Discussion started: 7 September 2022
© Author(s) 2022. CC BY 4.0 License.

2015 at the Saint Johns Bridge and the St Johns Railroad Bridge, respectively (see also Annear et al., 2003).

Water temperature records from these different locations are combined together to obtain a 90 year record of in-situ T_w covering 64% of the 1881 to 2021 period (Table 1). Once-a-day measurements were adjusted to the daily minimum temperature, because most historical measurements were made in the morning. The adjustment, typically ~0.1 ^{o}C, was based on the monthly averaged differences between measurement time stamps and the daily minimum in modern, high resolution data (Table 1). The composite 1881– 2021record uses lower Willamette records when available, and the nearest data otherwise (if available). Records in Oregon City and further upstream were adjusted for spatial heating effects through the use of monthly averaged gradients observed between coterminous measurements from 2000– 2017. Most adjustments for spatial variability were minor (<0.3 ^{o}C), except for a few years (1962, 1983– 1984) in which the only available measurements were from the middle or upper Willamette River. Additional notes are included in Table 1, and the source of data in the composite are included in the data record (see supplement).

Additionally, we use T_w measurements from the lower Columbia River to check our model estimates (see section 2.4) during periods with no other data (Figure 1, Table 1). Water temperature was measured up to twice daily at Astoria from 1854– 1876 (Talke et al., 2020), approximately 24 km from the present-day mouth. Monthly estimates of T_w at Astoria, Tongue Point (Rkm 29) are available from 1925– 1964 (USC&GS, 1967), and daily records were obtained from 1940–42 (Moore, 1968) and 1949– present from the National Oceanographic and Atmospheric Administration. Before 1950, surface waters at Astoria were generally freshwater or brackish during typical flow conditions (Al-Bahadily, 2020, USC&GS, 1967), and therefore approximate river water temperatures. During the November– April rainy season, good agreement is found between model results and Astoria measurements, thus helping to validate the model. During other times of year, snow melt from the interior Columbia River basin dominates the river flow signal (e.g., Naik & Jay, 2011; Helaire et al., 2019), suppressing water temperature (see Results, Section 3). Additional information about the Astoria measurements is given in Talke et al. (2020) and Scott et al. (2022).

Monthly averages of the USGS, DEQ, and City of Portland data from 2009 to 2015 agree to within 0.1– 0.2 ^{o}C, indicating that modern measurements from the last two decades are consistent and of high quality. This comparison also shows that grab samples from the water surface compare favorably with other methods. Measurements by the USSS (1881– 1890) and USWB (1941– 1961) were made at a 1st-order weather station by trained professionals, and appear to be of high quality; however, little independent verification is possible. Evaluation of data from 1962 to the mid-1990s indicates some periods with lesser quality in which different measurements disagree with each other. For example, summertime measurements from a thermograph in Oregon City (1963– 1967) are as much as 1.8 ^{o}C higher (monthly average) with coterminous grab-samples; a smaller, but still significant, bias is found between Saint Johns Bridge measurements (1971– 1975) and grab-samples (Table 1). Since the typical difference between such measurements is reported to be <1 ^{o}F (0.56 ^{o}C) (Moore, 1967), some unknown issue occurred. The availability and quality of in-situ data informs our choice of model calibration periods and interpretation of model/data comparisons.

https://doi.org/10.5194/egusphere-2022-793
Preprint. Discussion started: 7 September 2022
© Author(s) 2022. CC BY 4.0 License.

Table 1: In-situ water temperature measurements used to obtain a composite record of daily minimum water temperature in Portland, 1881– 2020. Locations ordered based on start-date and originating agency.

Location	Originating agency	Short name	River km	Latitude	Longitude	Measurement Dates	Measurement Frequency	Precision	Bias Correction
Astoria Downtown[a]	US Coast Survey	A1	CR. 24	46.19	-123.829	6/1854– 10/1876	Various, usually 6:00 am and 6:00 pm daily	±0.03 °C	None applied
Stark Street, Portland[b]	US Signal Service	S1	21	45.519	-122.671	9/1881 – 11/1890	11:00 am daily	±0.3 °C	0.1 °C to 0.2 °C
Astoria Tongue Point	US CGS (pre-1973) & NOAA	A2	CR 29	46.207	-123.768	1/1925– present; daily to 1995, hourly 1995– present	Monthly 1/1925– 12/1964; Daily 11/1940– 6/1942, 01/1949– 12/1995; Hourly 11/1993– present	±0.2 °C before 1994; ±0.03 °C modern	None applied
Morrison Street Bridge, Portland[b]	US Weather Bureau	W1	21	45.517	-122.668	7/1941 – 10/1961	7:30 am daily (except Sunday)	±0.3 °C	0 °C to 0.2 °C
Lower Willamette River[d]	Oregon Department of Environmental Quality	D1	19– 21 (primarily)	Various	Various	1949– 2015; 2746 grab samples retained after quality assurance	6:00am– 12:00 pm; mode = 9:00 am. monthly in winter, once weekly in summertime	±0.1 °C	Median 0.1 °C; 90% corrections < 0.2 °C
Harrisburg	USGS Gauge 14166000		259	44.2704	-123.174	6/1961– 9/1987 10/2000– Present	Daily Max, Min & Mean	±0.05 °C	
Oregon City	USGS Gauge 14207770	U2	42	45.3578	-122.610	3/1963– 9/1967	Daily Max, Min & Mean	±0.05 °C	0.7– 1.8°C Diff. w/Grab samples during summer
Salem	USGS Gauge 14191000	SA	137	44.9442	123.0429	10/1963 – 9/1987	Daily Max, Min & Mean	±0.05 °C	
Saint Johns Bridge	USGS Gauge 14211805	U3	9	45.583	-122.759	10/1971– 9/1975	Daily Max, Min & Mean	±0.05 °C	0.6– 1.05 °C Diff. w/Grab samples during summer
Morrison Street Bridge, Portland	USGS Gauge 14211720	U1	21	45.5175	-122.669	11/1975– 9/1981 11/2001– 9/2005 01/2009– Present	Daily Max, Min & Mean through 2005. Every 30 minutes	±0.05 °C	None applied
Willamette Falls Fish Ladder[e]	Oregon Department of Fish and Game	O1	43	45.354	-122.618	01/1985– present	Not tabulated; Daily, with gaps	± 0.2 °C	-0.3 to 0.3 °C, based on monthly difference with Portland
Saint Johns Bridge[f]	City of Portland, BES	C1	9	45.585	-122.765	7/1992 – 9/1999	Every 30 minutes	± 0.01 °C	Very biased; not used.
Saint Johns Railroad Bridge[f]	City of Portland, BES	C2	11	45.5773	-122.747	9/1997– 9/2012	Every 15 minutes	± 0.01 °C	Averaged with USGS record
Albany	USGS Gauge 14174000	AL	192	44.6388	-123.107	08/2001– Present	Daily Max, Min & Mean	±0.05 °C	

Notes: Stations ordered by start date, with earliest measurements first. All times given in local standard time. Bias corrections are subtracted from raw measurements on a monthly basis to obtain daily minimum; a positive value indicates a downward adjustment. Coordinates provided in the North American Datum of 1983. The locations for the measurements at Stark Street, Astoria Downtown, Willamette Fish ladder and the City of Portland measurements are estimated based on available data. River km are the thalweg distance from the mouth of the Willamette, except for Astoria which is on the Columbia River.

Specific Footnotes: (a) Measurements obtained from US National Archives; see Talke et al., 2020; (b) Measurements obtained from National Centers for Environmental Information; (c) Data obtained from NOAA; Grab samples from 1925– 1995, approximately daily, generally between 10:00am – 1:00pm; median ~11:30 am.(d) Data obtained from US EPA Storet database. Measurements often made from bridges in the Portland Metro area, including the Hawthorne Bridge, the Steel Bridge, and SPSS Railway Bridge. Samples pre-1960 discarded because of lack of time stamp. Grab samples after 12:00 pm (noon) not considered to avoid afternoon heating signal. Pre-12:00 pm data adjusted to daily minimum on monthly basis based on modern USGS data. Measurements at 1– 3 day frequency in 1964– 1972; (e) Data from 1985– 1999 obtained directly from agency; post 1999 records available online. Based on a comparison using 2001-2004 data, an average warming of 0.2 to 0.3 °C occurs between Willamette Falls and Portland from July to September. A cooling of up to 0.3 °C occurs between March to May. Little variation occurs at other times; (f) Obtained directly from agency; pre-2000 data also obtained from Berger et al., 2004.

https://doi.org/10.5194/egusphere-2022-793
Preprint. Discussion started: 7 September 2022
© Author(s) 2022. CC BY 4.0 License.

2.2.2 Meteorological and Flow records

A nearly complete record of discharge in the lower Willamette River is available from 1893–present, with less certain estimates from 1853– 1892. Daily discharge is available from the USGS in Portland from 1972 to the present (USGS Gauge 14211720). Routed estimates of discharge are available for earlier periods from 1878 forward from Jay & Naik (2011), based on USGS measurements at Albany (USGS Gauge 14174000) and Salem (USGS gauge 14191000). Routed estimates pre-1893 are less certain, because of gaps in the record (Jay & Naik, 2011). Daily Portland water level measurements are available from 1876– present, and estimates of 30d averaged Portland water level are available from 1855– 1876 based on tidal measurements at Astoria (Talke et al. 2020). Nineteenth century measurements incorporate a substantial backwater effect from the Columbia River that historically varied from zero to as much as 10 m during some spring freshet events (see Helaire et al., 2019).

Records of daily maximum T_a from the Portland-Vancouver area were found in several sources (Table 2). Continuous daily weather records at Vancouver (1849– 1868) and Eola (1870– 1892) were measured by the USSS and were provided in digital form by the Midwestern Regional Climate Center (https://mrcc.purdue.edu/). Additional daily records from the USWB and the National Weather Service from Portland and Vancouver cover the 1874– present period and were obtained from NCEI.

Air temperature records were carefully evaluated for potential bias (e.g., caused by elevation differences) and consistency with each other (Table 2; see Figure 1 for locations). For example, the Vancouver record from 1895– 1965 is on average ~0.4 to 0.5 ^{o}C warmer than the downtown Portland record. The Portland Airport reading was <0.05 ^{o}C cooler than the downtown Portland Weather Bureau reading between 1940– 1948, on average. Thereafter, the Portland Weather Bureau record warmed more quickly, and was 0.54 ^{o}C warmer than the Airport from 1960– 1969. The modern Portland KGW record (1973– present), located at 48.5m above sea-level, is slightly cooler from 1991– 2020 (annually averaged daily maximum = 17.08 ^{o}C) than the Portland Airport (17.47 ^{o}C). Under standard atmospheric conditions, with a lapse rate 6.5 ^{o}C per 1000m, a difference of ~0.3 ^{o}C is expected between these records. Thus, we conclude that the measured difference between the stations is almost entirely explainable by elevation effects. After adjusting for mean biases, the root-mean-square error observed between the different Portland air temperature records is around 1– 1.1 ^{o}C from 1940– present. Daily maxima between Vancouver and Portland show more variability (RMSE of ~1.5– 1.6 ^{o}C), possibly because of small differences in climate. The influence of these small differences on our T_w model results are explored later.

https://doi.org/10.5194/egusphere-2022-793
Preprint. Discussion started: 7 September 2022
© Author(s) 2022. CC BY 4.0 License.

Table 2: Meteorological stations used to develop statistical models, and associated root mean square error (RMSE) of water temperature obtained for different calibration periods (annual, summer, and winter). The RMSE represents either the daily or monthly averaged difference with in-situ water temperature measurements, in degrees Celsius. Station Identification numbers (ID) are from the US National Weather Service. Measurement dates denote the time period that daily maximum temperature was recorded at the given location. The latitude/longitude value for Eola (near Salem, Oregon) is estimated. All stations except Vancouver are in Oregon.

Name	Station ID	Measurement Dates	latitude	longitude	Model Name	Calibration Period	RMSE Annual Calibration (ºC)	RMSE Summer Calibration (ºC)	RMSE Winter Calibration (ºC)	RMSE Annual (monthly avg) (ºC)	RMSE Summer (monthly avg) (ºC)	RMSE Winter (monthly avg) (ºC)
Portland Downtown	USW00024274	1874– 1902	45.5166	-122.6667	1881D	1881–1890	1.1	1.2	0.87	0.78	0.92	0.5
Portland Downtown	USW00024274	1902– 1973	45.5333	-122.6667	1941D	1941–1952	0.91	0.68	0.75	0.62	0.48	0.43
Portland Airport	USW00024229	1938– 2021	45.5958	-122.6093	1941A	1941–1952	0.91	0.66	0.78	0.6	0.46	0.42
Portland Airport	USW00024229	1938– 2021	45.5958	-122.6093	2000A	2000–2015	0.88	0.51	0.75	0.62	0.31	0.48
Portland KGW[2]	USC00356749	1973– 2021	45.5181	-122.6894	2000D	2000–2015	0.87	0.53	0.72	0.62	0.33	0.46
Vancouver, Washington[3]	USC00458773	1849– 1868 1891– 1966	45.6333	-122.6833	1941V	1941–1952	0.98	0.75	0.85	0.68	0.54	0.48
Eola	US Signal Service Observation	1870– 1892	44.9323	-123.1198	1881E	1881–1890	1.22	1.41	1.05	0.91	1.17	0.72

Notes:

1. The annual RMSE between measurements and the climatological average is 1.86, 1.46, and 1.43 ºC for the 1881– 1890, 1941– 1952, and 2000– 2015 calibration periods, respectively.

2. The 1973– 1999 measurement was at a slightly different location of (45.517W, -122.683E). The elevation of the 1973– present dataset is ~48.5m. The lapse rate for the standard atmosphere (6.5 ºC per 1000m) suggests that the difference to a measurement at sea-level is ~0.3 ºC. An observed difference in average daily maximum temperature at the Portland Airport (17.46 ºC, <10m relative to sea-level) and Portland KGW (17.07 ºC) between 2000– 2020 is therefore mostly caused by elevation differences.

3. The Dec. 1849– 1868 measurement at Fort Vancouver was made by the US Signal Service; the approximate location was 45.633N,- 122.65E, and was several km east of the 1891– 1966 measurement. The gauge was moved in 1966 to a higher elevation location with a known bias (Mote et al., 2002). The 1966– present data is therefore not used.

2.3 Advection-Diffusion equation

To develop our statistical model approach, understand its limitations, and motivate its form, we first consider the underlying physical dynamics. Heating and cooling of river water is governed by the Advection-Diffusion equation (ADE; e.g., Fischer et al., 1979). When vertical and cross-sectional variations in T_w are neglected, the 1-D ADE for T_w as a function of time t and along-channel coordinate x (positive downstream) reads:

https://doi.org/10.5194/egusphere-2022-793
Preprint. Discussion started: 7 September 2022
© Author(s) 2022. CC BY 4.0 License.

$$\frac{\partial T_w}{\partial t} = \underbrace{-u\frac{\partial T_w}{\partial x}}_{Advective\ Term} + \underbrace{\frac{\partial}{\partial x}\left(K\frac{\partial T_w}{\partial x}\right)}_{Diffusive\ Term} + \underbrace{\frac{H}{\rho c_p d}}_{Heating\ term}, \quad (1)$$

where K is a horizontal diffusion coefficient, u is river velocity, H is the sum of heat flux into or out of the system, d is the cross-sectionally averaged depth, and c_p is the heat capacity of water, and is approximately constant to within 1% for typical variations in T_w. This simple ADE does not consider groundwater flow, which cools the off-channel alcoves of the Willamette River during summer (Faulkner et al., 2020).

Scaling provides insight into the relative importance of the advection, diffusion, and heating terms, relative to the time rate of change $\frac{\partial T_w}{\partial t}$. Over a 12 hour time scale during the day, temperatures in summer are observed to vary by ~0.5 °C, yielding $\left(\frac{\partial T_w}{\partial t}\right)_{daily}$ ~10^{-5} °C/s. Over a month, larger changes of order 5 °C are observed, yielding $\left(\frac{\partial T_w}{\partial t}\right)_{monthly}$ ~2×10^{-6} °C/s. The time rate of change for daily and monthly time scales must be balanced by the terms on the right hand side of Equation (1). An evaluation of measurements suggests that:

- The diffusive term is negligible. Over most of the year, the monthly average of daily $\frac{\partial T_w}{\partial x}$ is << 10^{-5} °C/m, except from July– September when a monthly-averaged increase of 1– 2 °C per 100km is observed (Figure 2b). Using 100km as a typical length scaleand K ~1000 m²/s for the diffusive term, the $\frac{\partial}{\partial x}\left(K\frac{\partial T_w}{\partial x}\right)$ term is generally < 10^{-7} °C/s, much less than $\frac{\partial T_w}{\partial t}$.
- The nonlinear advective term is likely influential during summer, due to a positive $\frac{\partial T_w}{\partial x}$ (Figure 2b). During other seasons, river discharge can either cool or warm Portland water because of the presence of both negative and positive $\frac{\partial T_w}{\partial x}$ (Figure 2). Therefore, the net influence of the advective term on monthly averaged temperatures is likely small, though it may matter during weather events (such as a rain-on-snow event).
- Seasonal variations in discharge (Figure 2a) influence the magnitude of the advective term. During early summertime (June) conditions, Lee (1995) measured velocities of ~0.8 m/s in the upper Willamette; tidally averaged currents are typically 0.05– 0.1 m/s during the same period in Portland (USGS Gauge 14211720). Since discharge is smallest during August/September, the decrease in u counteracts the increase in $\frac{\partial T_w}{\partial x}$ in the advective term $u\frac{\partial T_w}{\partial x}$. Overall, considering typical magnitudes of u and $\frac{\partial T_w}{\partial x}$, we find that the advective term scales as 10^{-5} °C/s to 10^{-6} °C/s during the summer, depending on location.

- Based on the considerations above, the heating term is usually the leading order term that drives the time rate of T_w, as also found, for example, by Wagner et al., (2011).

https://doi.org/10.5194/egusphere-2022-793
Preprint. Discussion started: 7 September 2022
© Author(s) 2022. CC BY 4.0 License.

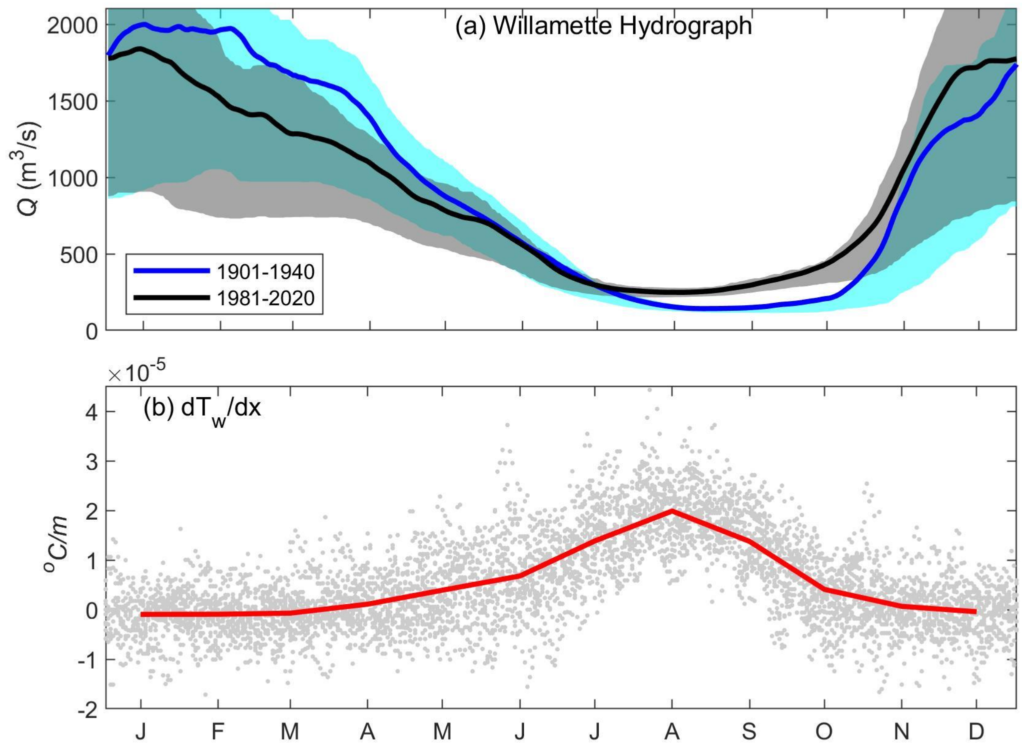

Figure 2: (a) The Willamette hydrograph at Portland, Oregon for the pre-reservoir (1901– 1940) and modern (1981– 2020) periods, and (b) the horizontal T_w gradient between Albany, Oregon and Portland Oregon for the 2000– 2017 time period. Positive indicates that downstream measurements in Portland are warmer. Shading in (a) denotes the 25th and 75th percentile of measured discharge. The along-river distance between Portland and Albany is 169 km. The red line in (b) denotes the monthly average. Tick marks denote the middle of each month.

When advection and diffusion are unimportant, the non-linear heating term ($\frac{H}{\rho c_p d}$) governs the time rate of change of temperature, $\frac{\partial T_w}{\partial t}$. The $\frac{H}{\rho c_p d}$ term can be linearized using a number of assumptions, enabling use of a linear regression approach in which T_w is a function of T_a and river discharge Q. The details, described briefly below, reveal some inherent limitations. See Mohseni & Stefan (1999) for a more detailed discussion of linearization assumptions.

First, we make the approximation that the reciprocal of depth, 1/d, is a function of Q:

$$\frac{1}{d} \approx a_1 - a_2 Q, \tag{2}$$

https://doi.org/10.5194/egusphere-2022-793
Preprint. Discussion started: 7 September 2022
© Author(s) 2022. CC BY 4.0 License.

where a_1 and a_2 are constants. The negative sign reflects the observation that 1/d decreases (depth increases) as discharge Q increases.

Further, the heat flux term is a function of at least 5 different terms (e.g., Fischer et al., 1979):

$$\sum \; H = H_s + H_e + H_{LW,gain} + H_{LW,loss} + H_{sw} \, . \tag{3}$$

The sensible heat flux is proportional to the difference between air temperatureT_a and T_w (both measured in Celsius):

$$H_s = k_1 w (T_a - T_w), \tag{4}$$

where k_1 is a constant that depends on air density and several empirical coefficients, and w is the wind speed at 10m. The energy loss because of evaporative heat flux, H_e, depends on wind speed, the latent heat of evaporation, and atmospheric conditions, and is generally small in winter but potentially significant in summer (Wagner et al., 2011). The third term, the heat input from radiation from water vapor, is

$$H_{LW,gain} = k_{LW,gain}(273.15 + T_a)^6 \propto k_{LW,gain} T_a \, , \tag{5}$$

Where $k_{LW,gain}$ is a constant that depends on cloud cover. When ΔT_a is small relative to $(273.15 + T_a)$, such as occurs in the Willamette, Equation 5 is approximately linear with respect to T_a . Similarly, heat loss due to long-wave radiation is modeled as

$$H_{LW,loss} = k_{LW,loss}(273.15 + T_a)^4 \propto k_{LW,loss} T_a, \tag{6}$$

where the power term is approximately linear in T_a for temperature differences < 20 degrees Celsius (see also Mohseni & Stefan, 1999). Finally, the heat input from incoming shortwave radiation, H_{sw}, is a function of sun angle, albedo, and atmospheric effects. Wagner et al. (2011) used the climatologically averaged insolation as a basis function in their T_w model, but most models implicitly assume that $H_{sw}\ R$ is proportional to T_a, (Benyahya et al., 2007).

Combining Equations 3 to 6, and neglecting the evaporation term, we find that H can be linearized as follows:

$$\mathrm{H(t)} \approx b_1 T_a + b_2 T_w + b_3 + error, \tag{7}$$

where b_1, b_2, and b_3 are constants.

Combining Equation 7 and Equation 2, the heating term can be approximated by:

$$\frac{H}{\rho c_p d} \approx c_1 T_a + c_2 T_w - c_3 Q T_w + c_4 Q T_a + \epsilon, \tag{8}$$

Where ϵ is the approximation error and c_1, c_2, c_3, and c_4 are coefficients. Equation 8 shows that even after many simplifications and approximations, there are still nonlinear interactions between terms such as air temperature and river flow (i.e., the QT_a term). In practice, it is found

https://doi.org/10.5194/egusphere-2022-793
Preprint. Discussion started: 7 September 2022
© Author(s) 2022. CC BY 4.0 License.

or assumed that air temperature is the most important factor in heating, and only the T_a dependence is retained (e.g., Erickson & Stefan, 2000, Webb et al., 2003). Most statistical models implicitly start with this assumption, though some non-linear regression approaches have been applied (see review by Benyahya et al., 2007). For our purposes here, we note that simplifying heating to be a linear function of T_a works best during periods of relatively constant water temperatures and river discharge (see also Mohseni & Stefan, 1999). This is one reason why models calibrated to a specific season such as summer often works better than a model fit to an entire year (see below).

The advection term in Equation 1 can similarly be linearized by assuming that either $\frac{\partial T_w}{\partial x}$ or Q is constant or slowly varying, relative to the other. This yields either a regression term in Q or in T_w. Removing nonlinear terms, the following linearized basis function emerges:

$$\frac{\partial T_w}{\partial t} = b_w T_w + b_a T_a - c_Q Q, \tag{9}$$

where b_w, b_a, and c_Q are coefficients and the minus sign indicates that river flow reduces water temperature. Using the approximation $\frac{\partial T_w}{\partial t} \approx \frac{T_{w_n} - T_{w_{n-1}}}{\Delta t}$, we find that T_w at time step n is equal to the T_w at the previous time step n– *1*, plus a correction that is a function of T_a and Q:

$$T_{w_n} = T_{w_{n-1}} + \Delta t b_w T_{w_n} + \Delta t b_a T_a - \Delta t c_Q Q \tag{10}$$

This is an autoregressive (AR1) process. Hence, at time n– *1*, T_w is a function of the T_w at time n– 2, and the T_w at n– *2* depends on T_w at n– *3*. If we develop and then substitute the solutions for $T_{w_{n-1}}, T_{w_{n-2}}, \ldots$. into Equation 10, we find that

$$T_w(t) = \sum_{\tau=0}^{\tau=j} a_\tau(t-\tau) T_a(t-\tau) + \sum_{\tau=0}^{\tau=j} b_\tau(t-\tau) Q(t-\tau) + C, \tag{11}$$

where a_τ and b_τ are regression coefficients at some time lag τ, C is a constant of regression, and the time period j is chosen to be long enough that the coefficients a_τ and b_τ effectively become negligible and/or statistically insignificant. The coefficients a_τ and b_τ can be modeled using an exponential filter approach (e.g., Al-Murib et al., 2019); here, as explained below, we estimate the coefficients directly. At a large time lag, the influence of the time-lagged temperature term in Equation 10 becomes negligible and drops out; hence Equation 11 effectively represents T_w as a function of time lagged T_a and river discharge.

The discussion above suggests that linear regression models have a basis in the underlying physical dynamics (see also Mohseni & Stefan, 1999). However, a number of assumptions and approximations must be made to represent the 1D ADE as a linear model. Factors such as wind, evaporation, time or spatial variation in parameters and heating terms, and alterations in depth are only approximately represented by T_w and Q. Moreover, depending on conditions, different terms (e.g., depth, heat flux, and velocity) may contribute in varying degrees to the overall heat balance. Thus, a linearized representation of average conditions during a particular season may work less well under unusual or extreme conditions.

https://doi.org/10.5194/egusphere-2022-793
Preprint. Discussion started: 7 September 2022
© Author(s) 2022. CC BY 4.0 License.

2.4 Statistical Model

Statistical models are often used to interpret and predict T_w patterns, using a number of different regressions, statistical approaches, or machine learning (e.g., Benyahya et al., 2007, Zhu et al., 2018). Within the Pacific Northwest, many studies have developed statistical regression models which use T_a and sometimes also river discharge Q to model measured T_w (Moore 1967; Donato, 2002; Bottom et al., 2011; Mayer, 2012). Such models are simple and run quickly, enabling evaluation of time-periods for which in-situ measurements are unavailable and allowing interpretation of primary forcing factors.

We employ a stochastic modeling approach (e.g., Caissie et al., 1998; Benyaha et al., 2007) in which the dependent variable (water temperature T_w) and the independent variables (air temperature T_A and river discharge Q) are decomposed into a long term climatological average and a time varying component. A similar approach has also been applied to the Columbia River (Scott, 2020; Scott et al., 2022). For a generic variable X(t) measured daily, the climatological average is defined as,

$$\overline{X(t)} = \frac{1}{y_2 - y_1 + 1} \int_{y_1}^{y_2} \int_{-T/2}^{T/2} X(t)dt\, dy, \quad (12)$$

where T = 30 days, t is the integer number of days since the start of the year, y_1 is the beginning year of the time series (e.g., 1881), y_2 is the end year (e.g., 1890), and the overbar represents the climatological average. The number of years in the average should be long enough to capture natural variability, but short enough to be statistically stationary (i.e., not overly influenced by land use changes or climate change). The 95% uncertainty in the climatological average is given by $\frac{t_* \sigma}{\sqrt{N}}$, where $t_* = 1.96$ for a large sample size N, and σ is the standard deviation. In practice, the number of years we used to define the climatological average is limited by available data.

The deviation from climatology, caused for example by a heat wave, is defined as:

$$X'(t) = X(t) - \overline{X(t)} \quad (13)$$

The climatological average for water temperature, $\overline{T_w(t)}$, is a good first approximation for conditions at any given year-day, and correctly estimates daily T_w in Portland to within a root-mean-square-error (RMSE) of ~1.5 to 2 °C. For a model to have predictive and explanatory power, it must exhibit an RMSE significantly less than this climatological average. Present-day numerical models typically fulfill this criterion and have an RMSE <1°C (Dugdale et al., 2017). To obtain comparable error statistics, we rewrite Equation 11 in terms of deviations of T_w from climatology, and form the following basis function:

$$T_w'(t) = \sum_{\tau=0}^{\tau=j} a_\tau(t-\tau) T_a'(t-\tau) + \sum_{\tau=0}^{\tau=j} b_\tau(t-\tau) Q'(t-\tau) + C\,, \quad (14)$$

where the prime indicates a deviation from climatology and other terms are as defined in Equation 11. Based on experimentation, we use daily T_a' out to two weeks. Thereafter, we use average T_a', to obtain a statistically significant correlation. A 15 day average is used for day 15– 30, and 30 day averages are used thereafter, up to 6 months. Similarly, river discharge Q' is averaged

https://doi.org/10.5194/egusphere-2022-793
Preprint. Discussion started: 7 September 2022
© Author(s) 2022. CC BY 4.0 License.

using a 10 day average for day 1– 10, a 20 day average for day 11– 30, and – a 30 day average thereafter.

A total of 8 statistical models are developed, based on data from the 19th century (1881– 1890), mid-20th century (1941– 1952), and modern period (2000– 2015) (see Table 2). These periods were chosen based on available data; they approximate (nearly) pre-development conditions, pre-flood control conditions, and modern conditions. With-in each model, we further divide the year into a summer sub-model (July– September), a winter sub-model (January– March) and an annual model, based on all available data. Experimentation was used to obtain the optimal winter and summer models. For example, including June or October into the summer model significantly reduced goodness of fit and the statistical influence of river discharge, consistent with the observation that the horizontal temperature gradient is largest from July to September (Figure 2b). Through experimentation, we also determined that discharge only produces a statistically significant effect for summertime models based on 1941– 1952 and 2000– 2015 data. This result is consistent with previous studies (e.g., Isaak et al., 2012) and with estimates of $\frac{\partial T_w}{\partial x}$ (section 2.3, Figure 2) which suggests that discharge effects are most prominent in summer.

Results show that the best-fit coefficients generally decrease in magnitude as T_a (Figure 3a,b,c) and river discharge (Figure 3d) are lagged backwards in time. Further, the decorrelation structure is different for the 19th, mid-20th, and 21st century models (Figure 3); hence, for the same forcing, these statistical models will produce a different output. Statistically significant coefficients are found at up to 3 month lag in the 1880s model, and 4 months in the others.

https://doi.org/10.5194/egusphere-2022-793
Preprint. Discussion started: 7 September 2022
© Author(s) 2022. CC BY 4.0 License.

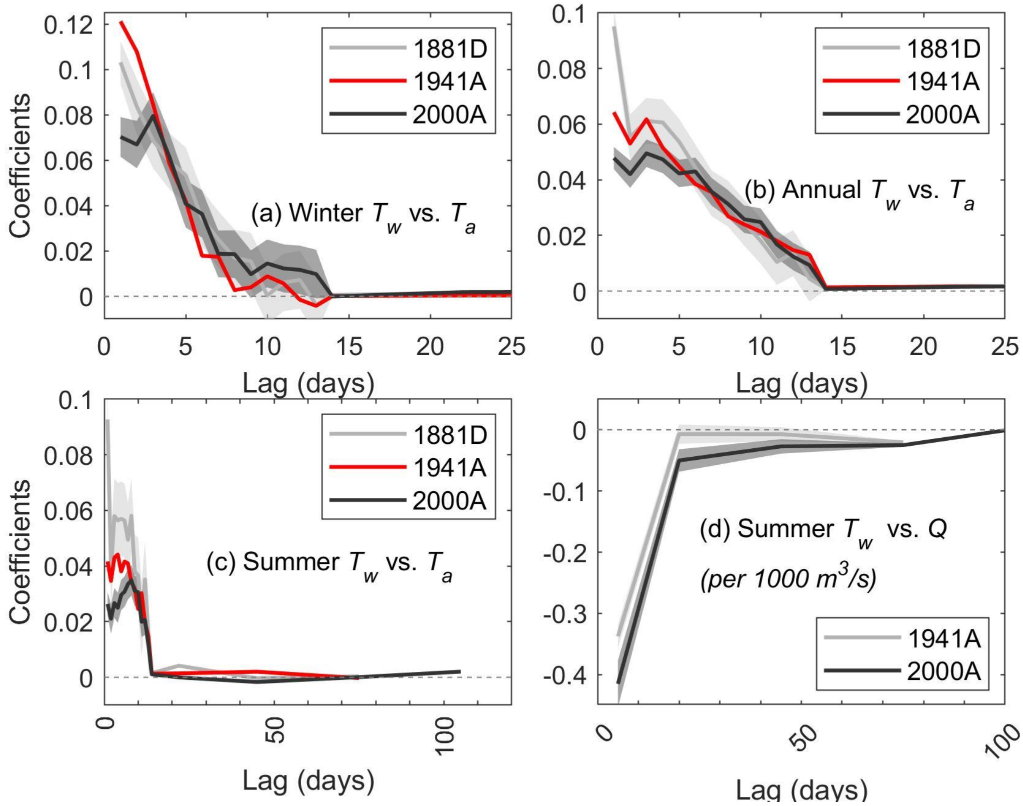

Figure 3: Coefficients for statistical model vs time lag for (a) air temperature (T_a) in the winter model (Nov– Mar); (b) T_a in the annual model (all months); (c) T_a in the summer model (July– Sept) and (d) discharge Q in the summer model (July– Sept). The 1881 model is calibrated to 1881– 1890 T_w data, the 1941 model is calibrated to 1941– 1952 T_w data, and the 2000 model is calibrated to 2000– 2015 T_w data. The letter denotes whether T_a data was sourced from Downtown Portland (D) or from the Airport (A). Similar results are found for the model based on Vancouver air temperature data (not shown). No statistically significant effect of river discharge was found for winter or annual models, and the 1880s summer model, and are not shown.

Each statistical model produces an estimate of T_w over the period of record of its underlying T_a record (Table 2; data available as supplemental information). Based on these time series, a composite estimate of modeled T_w was produced, as follows. First, for each station, estimates from the two seasonal sub-models were combined, with annual sub-model results used at other times. To avoid (typically small) discontinuities between sub-models, a 15-day linear relaxation period between sub-model start and stop times was applied. Next, a composite estimate for T_w was made for the 1850– 2020 period, using the best available meteorological measurements and statistical models. Vancouver measurements were used pre-1868, downtown Portland from 1874 to 1939, and the Portland Airport data thereafter. Water temperature estimated from Eola T_a measurements were used to fill the 1870– 1874 period. A compromise was required when deciding which era of model to use in the composite, since there is no clear delineation between pre and

https://doi.org/10.5194/egusphere-2022-793
Preprint. Discussion started: 7 September 2022
© Author(s) 2022. CC BY 4.0 License.

post-reservoir conditions, or between a nearly natural and substantially altered landscape. The mid-20th century calibration, representing pre-reservoir, post-landscape change conditions, was applied to the 1900– 1960 period; thereafter, we assume modern flood control, and applied the modern calibration. Pre-1900 estimates used the calibration based on 1880s data, except for the Vancouver period (1850– 1868), which used the mid-20th century model because there was no 19th century model. The validity of the composite modeled T_w is assessed, to the extent possible, through comparison with in-situ measurements (see Results).

Uncertainty was assessed by evaluating the root-mean-square error (RSME) between the composite model estimate and measurements, and comparing against the RMSE found using climatology. The uncertainty in each temperature estimate was assessed using a Monte Carlo approach. Two thousand possible ensembles of the model coefficients were created, under the assumption that coefficient uncertainty was normally distributed. The 95th percentile of the resulting spread of solutions is reported.

3.0 Results and Discussion

3.1 Model Assessment

Time-series comparisons of water temperature (Figure 4) and statistical evaluations (Table 2) confirm that the statistical model reproduces reasonably well year-to-year differences in T_w and weekly-monthly perturbations caused by persistent warm/cold weather. Some synoptic scale events of less than a week are only partially captured, possibly because of factors not included in the model (such as cloud cover, wind, or depth changes due to backwater from the Columbia River; see also Wagner et al., 2011) and the tendency of statistical models to underestimate extremes. The RMSE between the measured and modeled daily minimum T_w varies from 0.87 to 1.1 °C for the annual model, with RMSE as low as 0.53 °C and 0.72 °C for the summertime and wintertime models, respectively (Table 2). Results are less good using Eola, a weather station which is located ~70km from Portland and may imperfectly represent local meteorological forcing. On a monthly averaged scale, RMSE varies from ~0.3 to 0.9 °C, with the best agreement obtained during the modern period and the summertime sub-models (Table 2).

Our statistical model results compare favorably with numerical models; the RMSE at Portland for a calibrated numerical model based on measurements from April through September 2002 was 0.43 °C (Berger et al., 2004), compared to 0.52 °C for our model over the same period. Similarly, the model performs significantly better than estimates based on T_w climatology, which we calculate has a root-mean-square error (RMSE) of 1.86, 1.46, and 1.43 °C for the 1881– 1890, 1941– 1952, and 2000– 2015 calibration periods, respectively. We conclude that the statistical model accurately represents the most important factors affecting T_w, as long as the underlying measurements driving the model are reasonably accurate.

Modeled T_w estimates based on different T_a data series (Table 2) compare well with each other, with similar averages and variability. During their period of overlap from 1940– 1973, modeled water temperatures are slightly larger (0.08 °C) using the airport model (1941A) than the downtown Portland model (1941D). Similarly, the Vancouver model (1941V model) is 0.02 °C lower than the airport model (1941A) between 1940 and 1965. For the same periods, the daily RMSE

https://doi.org/10.5194/egusphere-2022-793
Preprint. Discussion started: 7 September 2022
© Author(s) 2022. CC BY 4.0 License.

between the 1941A model T_w and the 1941D and 1941V models is 0.29 °C and 0.32 °C, respectively. For the 1896– 1965 period, the 1941D and 1941V models show a mean difference of 0.06 °C (Vancouver larger), and an RMSE of 0.37 °C. These observations provide an order of magnitude estimate of the aggregate influence of input data and model variability on uncertainty, whether caused by spatial variations in T_a, differences in the statistical coefficients, or instrumental measurement uncertainty. The consistency and small RMSE between model results improves our confidence in results.

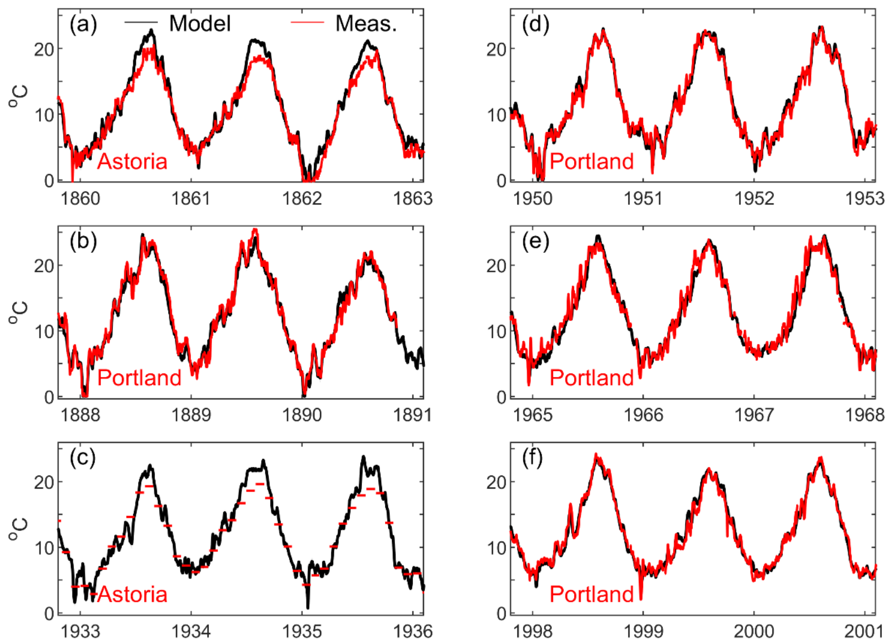

Figure 4: Comparison of modeled and measured T_w for six periods of three years. The composite Portland T_w is used in (b), (d), (e) and (f), while Astoria measurements are used in (a) and (c). Only monthly averages of T_w are available at Astoria from 1925 to 1940 and 1943– 1948 (see Table 1).

One of the factors driving the larger RMSE in the historical model is the larger overall system variance measured for T_w. The typical distribution of T_a anomalies from the climatological mean has remained stationary between different time periods, and the standard deviation is nearly the same (within ~5%; Figure 5). However, between the 1880s and the 2000– 2015 period, the distribution of measured T_w anomalies markedly contracted– , and the standard deviation decreased from 1.86 to 1.42 °C (Figure 5). Since the distribution of T_a anomalies remained similar, a likely explanation for the decreased variance in T_w is anthropogenic change to the local environment (e.g., flow regulation, landscape changes, system deepening), rather than changes in meteorological forcing (see below for further discussion).

https://doi.org/10.5194/egusphere-2022-793
Preprint. Discussion started: 7 September 2022
© Author(s) 2022. CC BY 4.0 License.

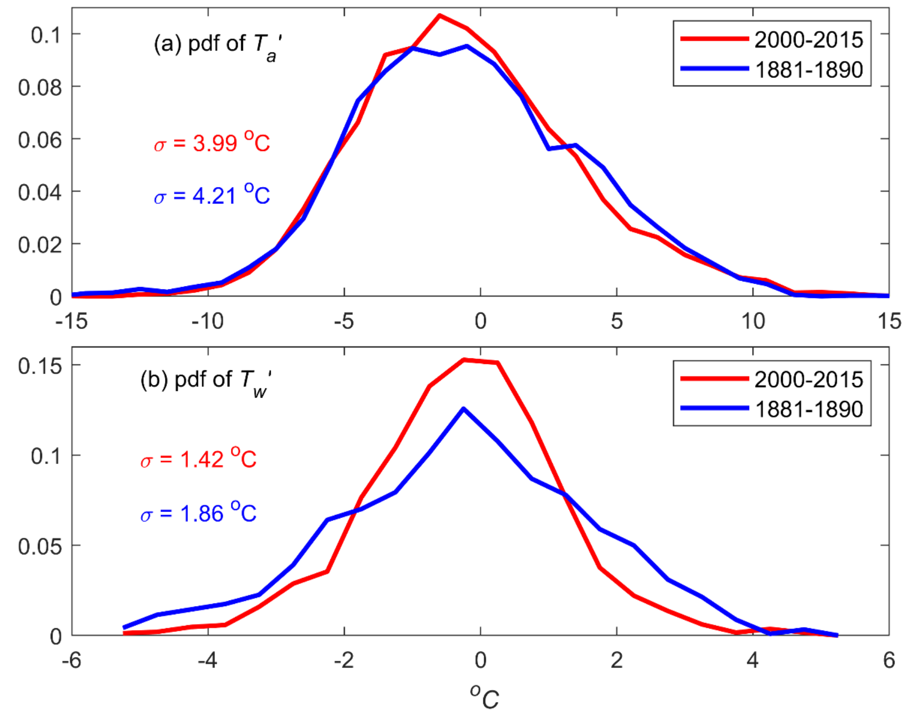

Figure 5: The distribution of T_a and T_w around the 30d climatological mean for the 1881– 1890 and 2000– 2015 periods.

3.2 Water Temperature Changes in lower Willamette

Model results and measurements show that water temperatures have increased steadily since the 1800s. Increases are observed at all times of the year (Figure 6), leading to an increase in annually averaged T_w of 1.1 ± 0.2 °C/century (Figure 7). The largest increase occurred in winter; during January– February, the trend in average T_w is 1.3 ± 0.3 °C/century (Figure 6a). Similarly, the minimum annual temperature is increasing quickly, at 1.8 ± 0.5 °C/century (Figure 7b). The smallest bi-monthly averaged trends occur in late spring, during May– June (0.82 ± 0.3 °C/century trend; Figure 6d). Maximum summer temperatures are trending upwards at ~0.9 ± 0.3 °C/century (Figure 7c), smaller than the annual average. Overall, model results (grey) track available in-situ measurements (red) well, except for some months during periods of lesser data quality in the 1960s– 1970s (Figure 6 & 7). Therefore, modeled and measured trends are consistent, increasing confidence in results.

https://doi.org/10.5194/egusphere-2022-793
Preprint. Discussion started: 7 September 2022
© Author(s) 2022. CC BY 4.0 License.

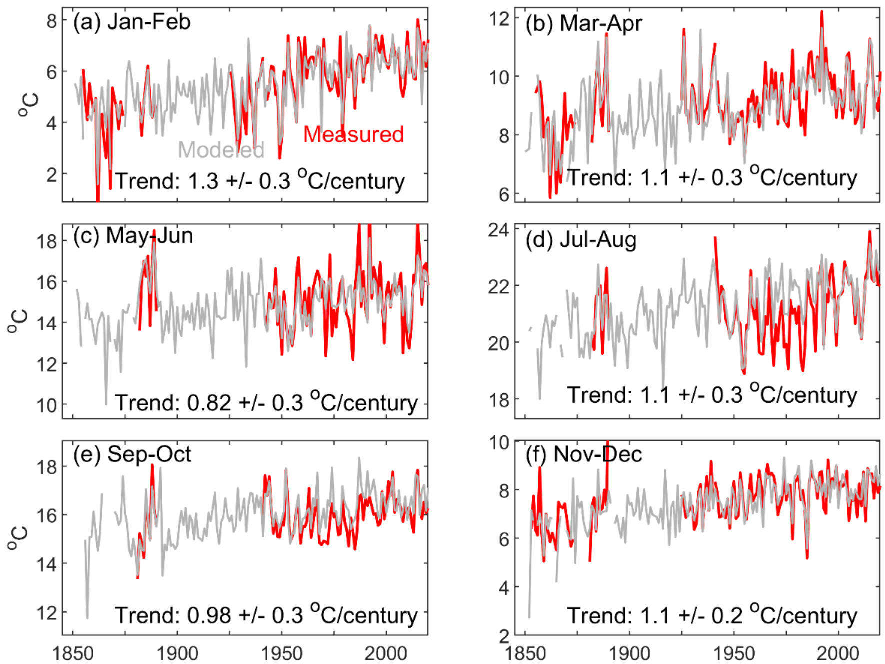

Figure 6: Seasonal trends in water level, averaged over two month water periods. A correlation is found between measurements (red) and model results (grey). Trends and 95% confidence interval based on a linear regression to model results, 1850– 2020. November– April data from 1854– 1876 from Astoria, Oregon (see Talke et al., 2020). Note different limits on the y-axis.

No single event or individual system perturbation appears to be causing trends, as there are no step-function changes or inflection points in T_w trends (Figure 6 & 7). Instead, an upwards tendency in T_w is interspersed by large year-to-year variability. In the modern system, the largest interannual variation occurs during the spring period (May– June), with swings of ~5°C observed between years (Figure 6). The late summer and autumn season (September– December) is least variable (order ~2 °C variability between years). Historically, greater year-to-year fluctuations occurred in both measurements and model results, particularly during the cooler half of the year (November– April). Cool-season measurements at Astoria (1854– 1876) between November and April confirm this variability, and track modeled results despite its location on the Columbia River (see e.g. Figure 4a and 4c). The correspondence occurs because during late fall and winter, proportionally more water in the lower Columbia is sourced from coastal tributaries, especially the Willemette, than during other times of year (see Naik and Jay, 2011 and Hudson et al., 2017).

Both climatic factors and system changes drive the reduction in interannual variability in T_w. Storage reservoirs, with a large thermal inertia, are one factor (see section 3.3). The change from a multi-braided, shallow channel to a single, deeper channel is also likely influential. Another reason for historical T_w variability in winter was the occasional occurrence of deep freezes that

https://doi.org/10.5194/egusphere-2022-793
Preprint. Discussion started: 7 September 2022
© Author(s) 2022. CC BY 4.0 License.

no longer occur. During the 1861– 62 and 1867– 1868 winters, for example, air temperatures remained below 0 ºC for 32 and 31 days, respectively, and newspapers recorded ice-skating on the lower Willamette River. Navigation in Portland Harbor was halted or hindered by ice from New Year's Day until mid-March, 1862. No 20th century winter matched the duration or severity of these events, though 18– 19 freezing days (maximum below 0 ºC) were recorded in 1915– 16, 1929– 30, and 1949– 50. In 1979, air temperatures remained below 0 ºC for a total of 14 days; since 1980, no winter has produced more than 9 sub-freezing days. Because some historical winters were mild (e.g., only one freezing day was recorded in 1862– 1863), historical water temperatures in winter were much more variable than today.

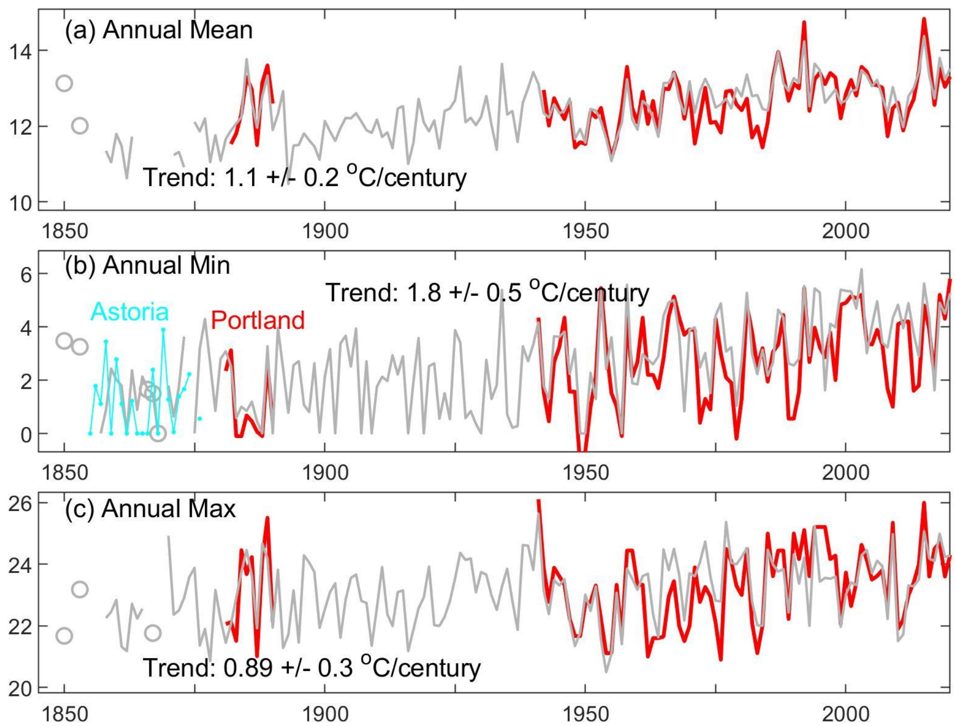

Figure 7: Time rate of change of annual mean, annual minimum, and annual maximum T_w. Grey denotes model data, red denotes data from Portland region, and cyan denotes T_w measurements in Astoria (annual minimum only). The trend is calculated by regression fit to the 1850– 2015 period. Evaluation is based on daily minimum T_w (see section 2). Years in the 1850s and 1860s without sufficient model data are excluded.

Results suggest that T_w has always exceeded a threshold of 20 ºC during summer for ~15– 90 days, even during the 1800s (Figures 4, 7c, 8 and 9). A spaghetti plot of all available in-situ data shows that most T_w measurements exceed the 20 ºC threshold in July and August (Figure 8).

https://doi.org/10.5194/egusphere-2022-793
Preprint. Discussion started: 7 September 2022
© Author(s) 2022. CC BY 4.0 License.

664 Peak temperatures typically occur during July or August, with no trend in timing observed (Figure 8, 9). The timing meteorological heat heat waves within a summer—which appears to be random—drives the timing of the peak. During some cool summers historically (e.g., 1949; see Figure 8), temperatures sometimes temporarily dipped below 20 °C during summer, and remained above the threshold for less than 2 months. In other years, T_w reaches a peak of 25– 26 °C, and water temperatures remain above the biologically important 20 °C threshold from June to September. During the hot, low river discharge summers of 1889and 2015 (Figure 8), water temperatures exceeded 20 °C for 91 and 95 days, respectively. The biggest difference, in line with other observations, is that T_w was more variable during the summer of 1889 than in 2015.

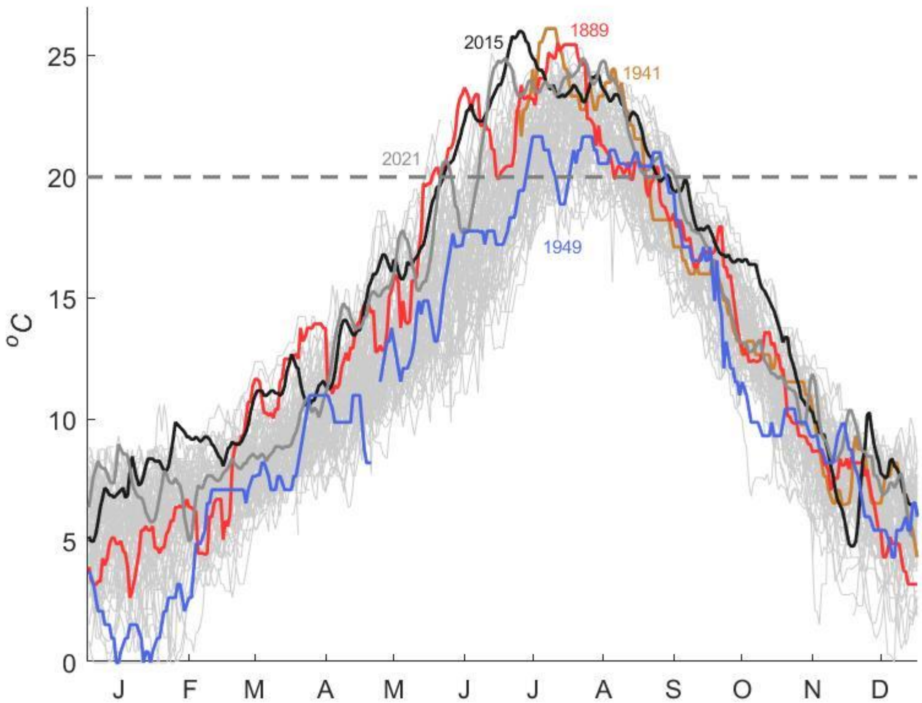

Figure 8: Spaghetti plot of all measured T_w data from between 1881– 1890 and 1941– 2021. Five years (1889, 1941, 1949, 2015, and 2021) are colored as labeled. Time is labeled at the midpoint of each month.

https://doi.org/10.5194/egusphere-2022-793
Preprint. Discussion started: 7 September 2022
© Author(s) 2022. CC BY 4.0 License.

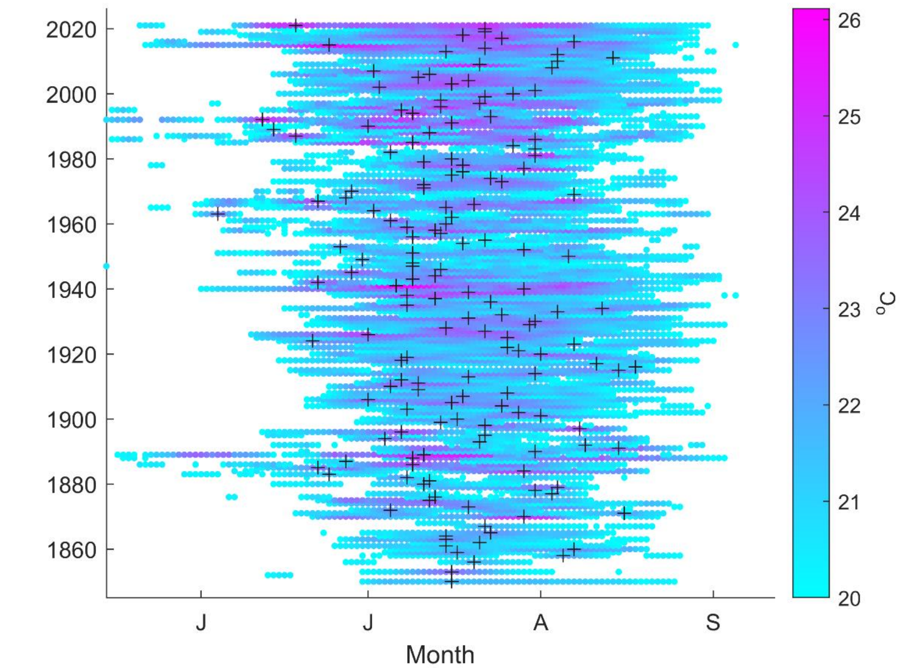

Figure 9: Summertime T_w values in the Willamette River that exceed a threshold of 20 °C, from 1850 to 2021. The instrumental record is used between 1881 and 1890 and 1941 to 2021, and the remainder is infilled with modeled T_w. Crosses denote the time of the peak annual T_w. Missing air temperature data precluded peak estimates for 1851– 1852, 1854– 1855, 1857, 1866, and 1868– 1869 (see supplemental data). Time is labeled at the midpoint of each month.

Summers with persistently elevated temperatures occur more often today, even though warm waters occurred in some historical years (Figures 8 & 9). Between 1881– 1890, measurements show that the 7-day average temperature exceeded the effective regulatory limit of 20.3°C (see Introduction) between 11– 80 days, with an average of 42 days. For the 2000– 2021 period, the range was 35– 92 days of exceedances, with an average of 63 days (2 months). The more consistently warm summer water temperatures help explain the observed upward trend in T_w (Figure 7). Interannual variability has also decreased, due in part to decreased sensitivity to synoptic (weather) related changes. Evaluated using a 10 year-average, the number of days per year that exceed 20 °C increased by roughly ~50% between 1850 and 2020, from around 40 d yr^{-1} to more than 60 d yr^{-1} (Figure 10), an increase of ~20 d. The threshold of 22 °C was exceeded relatively rarely in the 1800s (<5 days per year), but is now exceeded nearly 40 days per year. Before about 1960, there was more variability between decades than at present.

The number of cold-water days in winter has declined precipitously as overall temperatures have warmed (Figure 10a). Water temperatures are now rarely below 4 °C, compared to about 25 d

https://doi.org/10.5194/egusphere-2022-793
Preprint. Discussion started: 7 September 2022
© Author(s) 2022. CC BY 4.0 License.

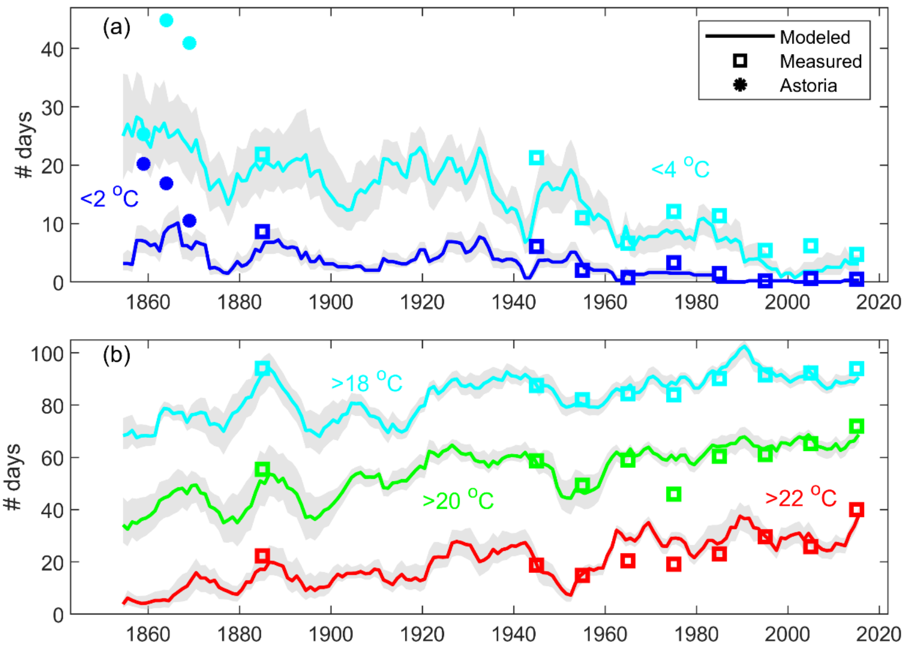

Figure 10: Comparison of the modeled and measured number of days per year from 1850 to 2020 that T_w is (a) below a threshold of 2°C and 4°C and (b) above thresholds of 18°C, 20°C, and 22°C. Square symbols denote the 10-year average based on measurements, while the solid line is a running 10 year average of modeled T_w. Measurements based primarily on bias corrected upstream gauges (1962, 1983–1984) are excluded. Grey shading is the 95% confidence interval, based on resampling model coefficients using a Monte-Carlo based technique. Wintertime measurements from Astoria (1854– 1876) included in (a).

per year in the mid-1800s. Similarly, near freezing temperatures (below 2 °C) were common in the 1800s (up to 10 d yr^{-1}), but almost never occur now. While an increase in winter water temperatures has received much less attention than summer-time trends, this shift is also ecologically important (e.g., Webb & Weber, 1993; Caissie, 2006). For example, cold water events and wintertime conditions influence the survivability and recruitment of fish by altering their biotic interactions, habitat use, physical condition, feeding rates, and community structure (see reviews by Hurst 2007; Brown et al., 2011; Weber et al., 2013). It is also possible that historical wintertime conditions, such as the deep freezes discussed above, provided some protection against non-native plants and fauna that thrive in warmer waters.

3.3 Interpretation of water temperature changes

In general, seasonal patterns of measured T_w and shifts between 19th and 21st century data are consistent with measurements of T_a, with some slight variations in timing and magnitude (Figure 11). Measurements in Portland indicate that the daily maximum air temperatures (T_a) increased

https://doi.org/10.5194/egusphere-2022-793
Preprint. Discussion started: 7 September 2022
© Author(s) 2022. CC BY 4.0 License.

by 1.3 °C between the 1875– 1904 and 1991– 2020 periods (Figure 11b), consistent with warming trends of 0.5– 2 °C per century at 100+ stations throughout the Pacific Northwest (Mote et al., 2003) and an average increase of ~1.1 °C since 1900 (Mote et al., 2019). The smallest increases in Portland T_a occur in spring (April– June) and in late fall (November– December), and the largest occur in January– February and July– October, again consistent with T_a trends in the Maritime Pacific Northwest (Mote, 2003). Within Portland, the large summertime increase may be influenced by the urban heat Island effect (e.g., Voelkel et al., 2018). However, the city has been relatively urbanized (cleared of forest) since the beginning of the time series, and T_a measurements have primarily occurred by either the Willamette or Columbia River, both reasons that changes in temperature bias caused by infrastructure may be relatively small. Moreover, the distribution of air temperatures around the climatological mean has remained virtually unchanged (Figure 5). Given the long history of Portland and later the Airport as the primary regional measurement station, and the consistency of trends with the regional average (e.g., Mote et al., 2019), we conclude that the T_a measurements are reasonably representative of regional climate patterns.

Average air temperatures during the 1881– 1890 calibration period (during the Signal Service T_w measurements) are only 0.4 °C cooler than the 2000– 2015 calibration period (Figure 11d), markedly lower than the 1.3 °C difference between the 30y climatological averages (Figure 11b). A possible reason is that pre-1888 measurements may not have been properly sheltered (Mote 2003). However, comparison with T_w measurements (compare Figure 11c with 11e) suggests that air and water temperature patterns during this decade were similar and warmer than previous and subsequent decades. For example, both springtime T_a and T_w measurements in the 1880s were higher than instrumental measurements from the 2000– 2015 period. The correspondence between T_a and T_w measurements in the 1880s increases confidence that measurements indicate a real climate signal, possibly caused by decadal fluctuations in climate (e.g., Peterson & Kinkel, 2001), rather than an instrumental artifact.

3.3.1 Causes of T_w Change

We next approximate the magnitude of factors causing T_w change using a series of sensitivity studies. These experiments provide an order-of-magnitude assessment of how sensitive the system is to changed coefficients or input data. We evaluate:

1. Integrated system changes. By applying the same input data to models from different time periods, we explore how the system response has changed to the same perturbations. River flow and T_a data from 2000– 2020 are used.
2. The effects of climate change. The climatological T_a increase since the 19th century in Portland is applied (Figure 11b), while river flow and the statistical model are kept the same.
3. The effect of water resources management. The change in the river hydrograph (Figure 2a) is applied, with the system coefficients and T_a held constant.

https://doi.org/10.5194/egusphere-2022-793
Preprint. Discussion started: 7 September 2022
© Author(s) 2022. CC BY 4.0 License.

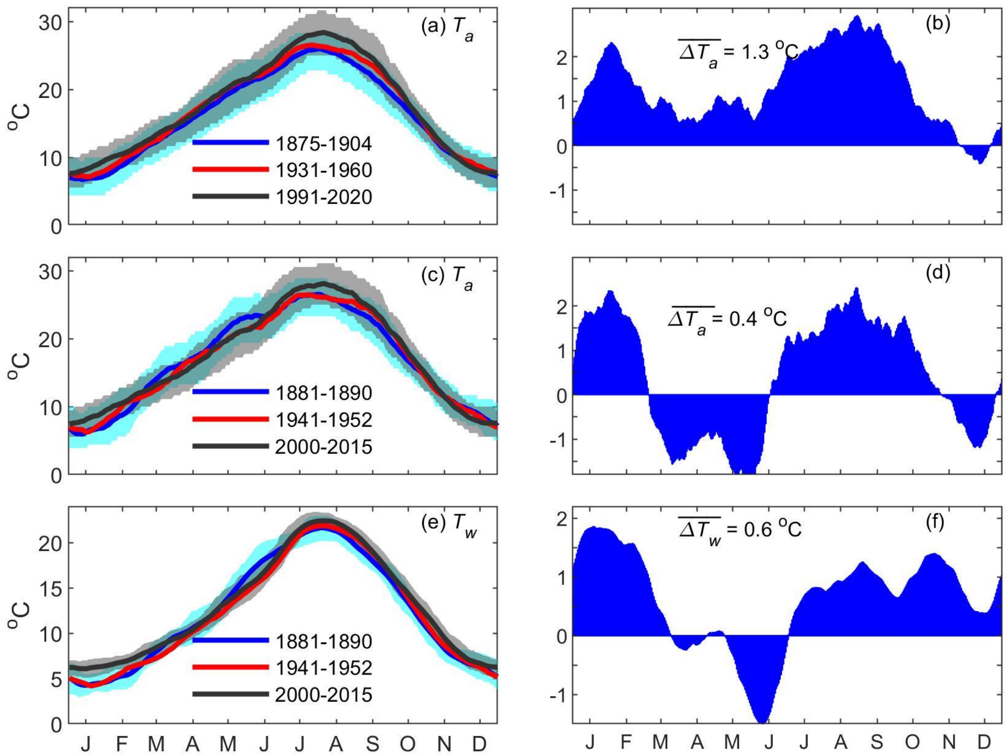

Figure 11: T_a and T_w climatology in Portland (a,c,e) and the difference between the modern (1991– 2020) and historical period (1881– 1890) in (b,d,e). Climatology is determined using a 30d moving average; shading denotes the 25th and 75th percentile of the measurements. A 30 year average is used in (a); the time periods for (c) and (e) are determined by the time period used to calibrate the T_w model. The tick marks on the x-axis denote the middle of each month. The average T_w difference between the modern and earliest period is provided in (b,d,e).

Model results confirm that changes in T_a (driven by climate change) are the most significant factor in long-term increases in T_w, with system changes an additional important contributor during the cool season (Figure 12). Seasonally, changes to T_a between the 1875– 1904 and 1991– 2020 periods dominate the modeled trends in T_w during summer and early fall (July– October) and in late winter (Figure 12). Averaged over a year, a total increase in T_w of 0.81 ± 0.25 °C is correlated to T_a changes. A maximum climate-induced change of ~1.7 ± 0.3 °C occurs in September. Climate shifts produce a lesser shift of 0.5– 0.6 °C increase in T_w in spring (late March to June), and little change occurs in December, consistent with air-temperature climatology (compare Figure 11 and 12). Interestingly, uncertainty in the air temperature contribution is driven by the inherent 95% confidence in the air temperature climatology, which is ±0.22 °C, rather than uncer-

https://doi.org/10.5194/egusphere-2022-793
Preprint. Discussion started: 7 September 2022
© Author(s) 2022. CC BY 4.0 License.

tainty in the model coefficients. Moreover, modeled T_w changes are robust to any small systematic biases in T_a; if the average change in T_a is reduced by 0.5 °C, the average T_w only decreases by ~0.3 °C. Hence, we conclude that changes to the meteorological heat-balance (as represented by T_a) are the major cause of increasing T_w. Climate models also suggest that future summertime T_w in the Pacific Northwest will increase much more than other seasons, consistent with our results (Ficklen et al., 2014).

System changes (as estimated by changing regression coefficients) between the 1940s and today cause a T_w increase of ~0.5– 0.6 °C from November– May, dropping to a statistically insignificant amount from late June to early October. Averaged over a year, the total increase in T_w caused by system change is 0.34 ± 0.12 °C. The observed seasonal shifts are consistent with an increased thermal inertia caused by the reservoir system, as also discussed elsewhere (see e.g. Webb & Weber, 1993; Caissie 2006; Olden and Naiman, 2010). Effectively, heating or cooling from many months ago still influences T_w in the modern system, tending to elevate wintertime and depress summertime temperatures (see discussion for other influences). In the statistical model, we find that monthly averaged T_a exerts a statistical influence on T_w for 4 months, compared to 3 months historically (not shown). The coefficient magnitudes at 2– 4 months lag are also larger today, at ~0.0025 $^oT_w/^oT_a$ per day (modern) vs. ~0.0017 $^oT_w/^oT_a$ per day (1940s; annual model). The other significant change in the modern model is a lessened sensitivity to synoptic weather patterns, as observed by smaller coefficients at <7 days lag (Figure 3) and less variance (Figure 5). Both the decreased sensitivity and the longer system memory in the modern system affect the modeled T_w, leading to the changed pattern of T_w responses to atmospheric forcing.

Changes in average river flow exert a minor influence on annually averaged T_w, but are important during late summer. During July, a slight increase in T_w is observed from changed river flow. In August and especially September, the decrease in T_w caused by increased flow releases, -0.27 °C and -0.56 °C are significant. Thus, the release of water from reservoirs late in the summer counteracts, to some extent, the effects of increased air temperatures. During other times of year, no statistically significant modeled correlation between Q and T_w was found, likely because the average T_w gradient in the mainstem Willamette River is small (Figure 2b). While river flow may be important in winter during times of large positive or negative temperature gradients, these changes are likely transient and a process-based model would be required to capture it. The net effect of summertime changes in river flow on the annual average is small: A total decrease in annually averaged T_w of ~0.05 °C is estimated.

https://doi.org/10.5194/egusphere-2022-793
Preprint. Discussion started: 7 September 2022
© Author(s) 2022. CC BY 4.0 License.

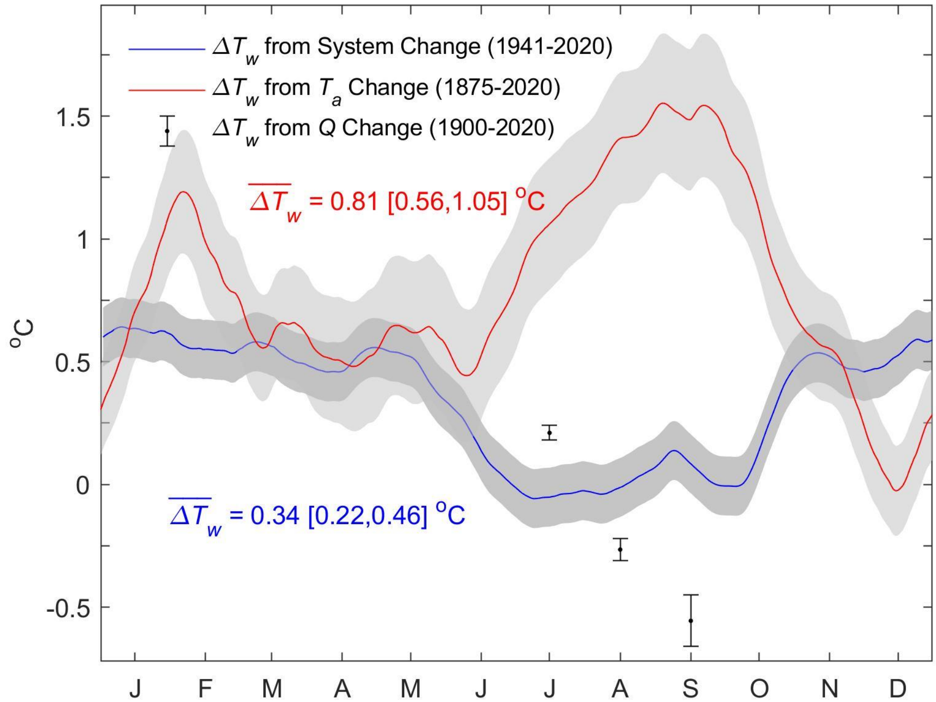

Figure 12: Estimated T_w changes caused by T_a (climate change), system changes (i.e., differences between the parameters of the modern and historic models), and discharge changes (July– September). A positive value indicates an increase over time. System changes are based on taking the difference in estimated T_w obtained over the 2000– 2020 time period using the 1940s era model (model 1941A) and the modern era model (model 2000A). The influence of increased solar heating (climate change) is estimated by differencing the T_a and T_w values obtained with the 1941A model using the 1875– 1904 and 1991– 2020 T_a climatologies (Figure 11). Shading includes the both the 95% uncertainty in the mean climatology and the 95% uncertainty in the coefficients. The July– September change in monthly averaged Tw produced by discharge is obtained by comparing the pre-reservoir (1901– 1940) and the modern (1981– 2020) hydrographs (Figure2a) into the statistical model, with T_a forcing held constant. The error bars denote the difference in the 1941A and 2000A model estimates.

Overall, the sum of estimated temperature changes caused by climate, system, and water management changes since ~1900 (~1.1 ± 0.3 °C; Figure 12) is consistent with the overall long-term trends in T_w of 1.1 ± 0.2 °C per century (Figure 7a). Thus, we conclude that ongoing climate change is the primary cause of increased temperatures, with system changes an important contributor. We note again that we cannot discern the influence of individual factors such as changed shading, river depth, storage, or snow pack, nor can we assess coupled, nonlinear

https://doi.org/10.5194/egusphere-2022-793
Preprint. Discussion started: 7 September 2022
© Author(s) 2022. CC BY 4.0 License.

changes. For example, changes to river flow may in part be caused by climate change, and alterations in T_a may in part be influenced by urbanization or deforestation. Nonetheless, the results provide insights into the causes of T_w change and why some parts of the year are subject to larger upward trends than others, over secular timescales.

4.0 Discussion

The observed annual trend in T_w of 1.1 ± 0.2 °C/ century in the lower Willamette River is similar to the magnitude of change observed or estimated in the few studies available over similar time scales. For example, Moatar and Gailhard (2006) estimated a 0.8 °C increase in the Loire since 1881, Webb and Noblis (2007) estimated a change of 1.4– 1.7 °C on Austrian rivers since ~1900, and Scott (2020) estimated a trend of 1.3 °C/ century for the nearby Columbia River over the past 170 years (see also Scott et al., 2022). Similar to our results, studies also often highlight that the seasonal distribution of changes of T_w is unequal (e.g.,,Webb and Noblis, 2007). Consistent with our results, studies from the Pacific Northwest suggest that climate change is driving T_w trends over recent decades (Isaak et al., 2012). Future climate change will continue to drive trends, with the largest increases in summer (Caldwell et al., 2013; Ficklin et al., 2014). But, our results suggest that system changes have altered the response of T_w to climate change, and in particular extremes, as explored below.

Both measurements (e.g., Figure 5) and the statistical model coefficients for T_a (Figure 3) suggest that the sensitivity of T_w to short-term meteorological forcing has decreased over time. A major cause is the reservoir system, which is known to decrease T_w variability in the Willamette on 1– 8 day time scales (Steel and Lange, 2007). At short time lags of 0–5 days, historical model coefficients are as much as 2–3x larger than modern coefficients (Figure 3). Therefore, a historical heat wave in T_a was likely to produce a larger change in T_w than today. Simultaneously, the integrated effect of weather during previous months is more important. At lags of > 2 weeks, coefficient magnitudes are ~50% larger in the modern models than historically. Hence, the thermal memory of the system to T_a anomalies lasting a month or longer is larger. Thermal memory stems from storage effects, whether from the heat stored in reservoirs (Webb & Weber, 1993; Caissie, 2006; Olden & Naiman, 2010) or the cooling effects of snow melt and groundwater in summer, which together are the primary source of water during this period (Brooks et al., 2012). The net thermal memory has increased, providing a buffering effect that helps explain why both seasonal and interannual variations in T_w are less pronounced today.

We attribute the decreased sensitivity of T_w to short-term, synoptic weather patterns (< 1 week) to a system-wide increase in depth, caused by the reservoir system (Rounds, 2007,2010) and by channelization and depth increases in the river (Sedell & Froggatt, 1984; Gregory et al., 2002a) A larger depth d decreases the magnitude of the heating term ($\frac{H}{\rho c_p d}$) in Equation (1), leading to smaller temperature change in the leading order balance $\frac{\partial T_w}{\partial t} = \frac{H}{\rho c_p d}$. This explains the decrease in model coefficients for small time lags (< 1 week). Reservoirs in the upper watershed increase the mean depth of the entire system, reducing the overall rate of temperature change but increasing heat storage capacity (Caissie, 2006). Similarly, the transition from a multi-braided stream to a dredged river with one primary channel also contributes to increased depth, to an unknown extent. Gravel mining and dredging for the harbor may also have increased depths in the lower

https://doi.org/10.5194/egusphere-2022-793
Preprint. Discussion started: 7 September 2022
© Author(s) 2022. CC BY 4.0 License.

Willamette (see e.g., Jay et al., 2011). These Portland-region depth increases may be offset by a decrease in backwater effects from the Columbia River, particularly in spring (Helaire et al., 2019).

The changing correlation structure (Figure 3) and the influence of increasing depth has implications for how climate change effects are observed. At short time scales (<1 week), the decreased modern sensitivity to air temperature perturbations (Figure 3) implies that depth increases outweigh altered H in the heating term. If the correlation structure had remained unchanged, a 1 ^oC step increase in T_a would result in a larger short-term perturbation than is currently observed. Hence, T_w in the modern system has become more resilient to extreme heat waves. The record breaking heat wave in July 2021, with a high T_a of 46.7 ^oC, did not cause a record T_w. Despite air temperatures exceeding the previous all-time high by ~5 ^oC, the daily minimum water temperatures peaked just over 24 ^oC, in part because the heat wave was shorter than other events. We conclude that water temperatures are now more influenced by climate-change induced changes to air temperature climatology and long-time scale patterns, rather than short-term extreme events.

Numerical, process based models run over a smaller time scale provide additional clues to the factors driving long-term changes. For example, non-reservoir anthropogenic factors were modeled to increase Willamette River water temperatures in Portland by 0.3 ±0.05 ^oC between June and October of 2001 (OR DEQ, 2006), primarily due to loss of shading (86%) and secondarily because of point-source discharges (e.g., from water treatment plants). The same CE2-Qual model determined a reduction of approximately 0.1 ^oC for each additional 100 m^3/s of river flow-released into the lower Willamette. This is consistent with our modern statistical model, which suggests an influence of ~0.07 ^oC for each extra 100 m^3/s of river flow, spread out over several months via the decorrelation structure (Figure 3d).

River flow effects on T_w are likely driven by the substantial positive summertime $\frac{dT_w}{dx}$ (Figure 2b) during July-September, but are also influenced by the increased velocity and depth caused by each incremental increase in discharge (see Equation 1). The large increase in September discharge (Figure 2) reduces temperatures by 0.56 ^oC, a larger amount than in August (Figure 12). In October, average $\frac{dT_w}{dx}$ becomes small (Figure 2), and our approach is unable to find a statistically significant influence of river discharge.

Interestingly, the overall system was less sensitive to river flow fluctuations in the 1940s (Figure 3d), and no statistically significant effect was observed in the 1880s. The lack of correlation in the 1880s may simply reflect imperfect flow estimates (see Jay & Naik, 2011). Nonetheless, it is possible that the bottomland forests and braided river networks of the historical Willamette River greatly reduced $\frac{dT_w}{dx}$, velocity, and the advective heating term during summer (Equation 1), producing the observed lack of correlation. Mechanisms that might be influential include stream width changes (e.g., White et al., 2017) and cold groundwater discharges, which is known to occur in off-main channel alcoves (e.g., Faulkner et al., 2020). During winter, the shallower historical streams may have contributed to the freezing water temperatures observed during some years in the 19th century. A process-based retrospective model using historical bathymetry would be required to further investigate these conjectures, and determine the relative roles of geomorphic change, ecological change, and the reservoir system on T_w.

https://doi.org/10.5194/egusphere-2022-793
Preprint. Discussion started: 7 September 2022
© Author(s) 2022. CC BY 4.0 License.

Since spring T_a values are less changed than summer values (Figure 11), less extra heat is input at the beginning of the warm season, and warm T_w is not biased early in the modern record. In the late summer, reservoir releases are tamping T_w values downwards (Figure 12).

The increase in the number of days that temperatures exceed a threshold has been observed in other river systems (e.g., Markovic et al., 2013) and is projected to continue in the Pacific Northwest (Mantua, 2010). Our observations show that the rate of change is threshold dependent, and slows as the accumulated number of days above a threshold becomes large. Therefore, the number of days over 20 ^{o}C (which is already large) is increasing less quickly than the number of 22 ^{o}C days, which occur primarily during mid-summer (Figure 9). Effectively, exceedences of lower thresholds like 18 ^{o}C and 20 ^{o}C are limited by spring and fall, when temperatures change quickly. Conversely, in winter, the largest rates of change are observed for larger levels of exceedance; hence, the number of cold-water days below 4 ^{o}C is decreasing faster than those below 2 ^{o}C. Average temperatures in Jan-Feb, the period with the coldest temperatures, have increased from ~0-6 degrees to 5-8 degrees (Figure 6a). Hence, both the decreased spread in temperatures (Figure 5) and the increased mean drive the large change in the number of days below 4 ^{o}C.

Compared to historical norms, water temperatures today exhibit less variability, both day-to-day and between the maximum and minimum (both climatology and daily extrema). A result is that *temporal refugia*—which we define as time periods in which water temperatures temporarily dip below biologically important thresholds such as 18 ^{o}C or 20 ^{o}C—are becoming less frequent (see Figure 9,10). Hence, while the management practice of selectively releasing river water is successfully reducing average temperatures in late summer (Figure 12), it may not be addressing the decrease in variance (e.g., Figure 5) caused by system changes. Because some migrating fish such as steelhead delay migration during warm periods by weeks or months, likely causing increased mortality (e.g., Siegel et al., 2021), the reduced temporal refugia are important to consider (see also Steel et al., 2012). At Portland, T_w exceeds—and has done so throughout the period of record—biologically important thresholds during some part of every year. However, the more consistently warm temperatures during summer and the shoulder seasons—as observed by the increase in the time over 18 ^{o}C and 20 ^{o}C—likely creates a thermal barrier that has implications for salmon migration (see e.g., Notch et al., 2020). .

5.0 Conclusion

In this contribution, we found, digitized, produced, and quality controlled a long T_w record (1881– 1890, 1941– 2021) for the lower Willamette River in Portland, Oregon. The in-situ measurements enabled the development of statistical T_w models based on the 1880s, 1940s, and modern time periods. Subsequently, estimates of daily minimum T_w for the years 1850– 2021 are produced using daily measurements of T_a and river discharge. A good comparison between measurements and models is observed (Table 2), including cool season water temperature measurements (November – April) in the Columbia River Estuary from 1854– 1876.

Water temperatures are increasing throughout the year (average trend of 1.1 ± 0.2 ^{o}C/ century), with the largest trends observed in winter. As a result, the number of cold water days per year is precipitously declining, while the number of days above 20 ^{o}C has increased by an average of ~20 d yr^{-1} (Figure 10). The primary cause of changed T_w since ~1900 is climate change (0.84 ^{o}C), followed by system changes such as the building of reservoirs, loss of shading, and other

https://doi.org/10.5194/egusphere-2022-793
Preprint. Discussion started: 7 September 2022
© Author(s) 2022. CC BY 4.0 License.

landscape alterations (0.34 °C; Figure 12). Changes and reductions in flow have a generally smaller influence. Because of a larger heat capacity and greater system depth, the day-to-day variability in T_w has decreased (e.g., Figure 5). Even though average temperatures in summer are now larger, peak temperatures have changed less. Hence, warm summers marked by low river flow produced similar peak temperatures in 1889, 1941, and 2015 (Figure 9), and a truly extreme heat wave in 2021 did not produce record water temperatures, possibly because of its short duration. The relative suppression of peak T_w has been bought at the expense of daily and interannual variability; during most times of the year, but particularly in winter, there is less day-to-day variation than in the 19th century. Climatic induced disturbance events such as freezing rarely occur anymore. Similarly, temporal refugia—time periods in which T_w dips below biologically important thresholds—have also decreased (Figures 9 & 10). These system changes may pose a grave threat to endemic species, should climate-induced changes in T_w continue.

Data Availability

The water temperature data used in the research is available upon request, and will be uploaded to a data repository upon acceptance of the manuscript. Meteorological data are available from the National Centers for Environmental Information (https://www.ncei.noaa.gov/). Pre-1890 Vancouver and Portland records were also obtained from the Midwestern Regional Climate Center (https://mrcc.illinois.edu/data_serv/cdmp/cdmp.jsp). River flow records are obtained from the US Geological Survey and the sources described in section 2.

Author Contribution

SAT found and processed archival data, developed the statistical model, analyzed results, produced figures, and was primary lead on drafting the paper. DAJ developed an earlier version of the model and assisted with interpretation and paper development. HLD assisted with interpretation and paper drafts, and helped secure funding.

Competing Interests

The authors declare that they have no conflict of interest

Acknowledgements

Funding was provided by Bonneville Power Administration, under Project No. 2002-077-00 with the Pacific Northwest National Laboratory, and by the US National Science Foundation, CAREER Award 1455350 and NSF project 2013280. Margaret McKeon is thanked for her help defining the watershed boundaries in Figure 1, and students at Portland State University are thanked for helping to digitize and quality assure the 1854-1876, 1881-1890, and 1941-1961 water temperature records used in this study.

https://doi.org/10.5194/egusphere-2022-793
Preprint. Discussion started: 7 September 2022
© Author(s) 2022. CC BY 4.0 License.

References

Al-bahadily, A.: Long Term Changes to the Lower Columbia River Estuary (LCRE) Hydrodynamics and Salinity Patterns. PhD thesis. Portland State University, doi: 10.15760/etd.7357, 2020.

Al-Murib, M. D., Wells, S. A., and Talke, S. A.: Integrating Landsat TM/ETM+ and numerical modeling to estimate water temperature in the Tigris River under future climate and management scenarios. Water, 11(5), 892, doi.org/10.3390/w11050892, 2019.

Angilletta M.J., Steel E.A., Bartz K.K., Kingsolver J.G.,Scheurell M.D., Beckman B.R., and Crozier L.G.: Big dams and salmon evolution: changes in thermal regimes and their potential evolutionary consequences. Evolutionary Applications,1, 286–299, doi: 10.1111/j.1752-4571.2008.00032.x, 2008.

Annear, R., McKillip, M., Khan, S. J., Berger, C., and Wells, S.: Willamette Basin Temperature TMDL Model: Boundary Conditions and Model Setup, Technical Report EWR-03-03, Department of Civil and Environmental Engineering, Portland State University, Portland, Oregon, 2003.

Baker, J., Van Sickle, D., White, D.: Water Sources and Allocation. In: Willamette River Basin Planning Atlas (D. Hulse, S. Gregory and J. Baker, Eds.), pp. 40–43. Oregon State University Press, Corvallis, 2002.

Benyahya L., Caissie,D.,St-Hilaire, A., Ouarda, T.B.M.J., and B. Bobée.: A Review of statistical water temperature models. Canadian Water Resources Journal. 32(3): 179-192, doi.org/10.4296/cwrj3203179, 2007.

Benner, P., and Sedell, J.: Upper Willamette River Landscape: A Historic Perspective. in River Quality : Dynamics and Restoration. Ed. Antonius Laenen and David A. Dunnette. Boca Raton: CRC/Lewis, 23-46, 1997.

Berger, C., McKillip, M.L., Annear, R.L., Khan, S.J., and Wells, S.A.: Willamette Basin Temperature TDML Model: Model Calibration. Portland State University, Department of Civil and Environmental Engineering. Technical Report EWR-02-04, 2004.

Branscomb,A., Goicochea J., and Richmond, M.: Stream Network. In: Willamette River Basin Planning Atlas (D. Hulse, S. Gregory and J. Baker, Eds.), pp. 16-17. Oregon State University Press, Corvallis, 2002.

Brooks, J. R., Wigington, P. J., Phillips, D. L., Comeleo, R., and Coulombe, R.: Willamette River Basin surface water isoscape (δ 18O and δ 2H): temporal changes of source water within the river, Ecosphere, 3, 39, doi:10.1890/ES11-00338.1, 2012.

Brown, R. S., Hubert, W. A., and Daly, S. F.: A primer on winter, ice, and fish: what fisheries biologists should know about winter ice processes and stream-dwelling fish. Fisheries, 36(1), 8-26, doi.org/10.1577/03632415.2011.10389052, 2011.

Bumbaco, K. A., Dello, K.D., and Bond, N.A.: History of Pacific Northwest Heat Waves: Synoptic Pattern and Trends. Journal of Applied Meteorology and Climatology, DOI:10.1175/JAMC-D-12-094.1, 2013.

Bottom, D., Baptista, A., Burke, J., Campbell, L., Casillas, E., Hinton, S., Jay, D.A., Lott, M. A., McCabe, G., McNatt, R., Ramirez, M., Roegner, G. C., Simenstad, C. A., Spilseth, S., Stamatiou, L., Teel, D. and Zamon, J. E.: Estuarine habitat and juvenile salmon: Current and historical linkages in the Lower Columbia River and estuary. Final report, 2002-

https://doi.org/10.5194/egusphere-2022-793
Preprint. Discussion started: 7 September 2022
© Author(s) 2022. CC BY 4.0 License.

2008. Report of the National Marine Fisheries Service to the U.S. Army Corps of Engineers. Portland, Oregon. Available at https://www.nwfsc.noaa.gov/publications/index.cfm, 2011.

Boyd, Robert, ed. Indians, Fire, and the Land in the Pacific Northwest: Corvallis: Oregon State University Press, 1999.

Caissie, D., El-Jabi, N. and St-Hilaire, A.: Stochastic Modelling of Water Temperatures in a Small Stream Using Air to Water Relations. Canadian Journal of Civil Engineering, 25: 250–260, doi.org/10.1139/l97-091, 1998.

Caissie, D.: The thermal regime of rivers: a review. Freshwater Biology, 51: 1389-1406, doi.org/10.1111/j.1365-2427.2006.01597.x, 2006.

Caldwell, R.J., Gangopadhyay, S., Bountry, J., Lai, Y. and Elsner, M.M.: Statistical modeling of daily and subdaily stream temperatures: Application to the Methow River Basin, Washington. Water Resources Research. 49: 4346 – 4361, doi.org/10.1002/wrcr.20353, 2013.

Chang, H., and Jung, I. W.: Spatial and temporal changes in runoff caused by climate change in a complex large river basin in Oregon. Journal of Hydrology, 388(3), 186-207, doi.org/10.1016/j.jhydrol.2010.04.040, 2010.

Christy, J.A. and Alverson, E.R., 2011. Historical vegetation of the Willamette Valley, Oregon, circa 1850. Northwest Science, 85(2), pp.93-107.

Crozier, L. G., Siegel, J. E., Wiesebron, L. E., Trujillo, E. M., Burke, B. J., Sandford, B. P., & Widener, D. L.: Snake River sockeye and Chinook salmon in a changing climate: implications for upstream migration survival during recent extreme and future climates. *PloS one*, *15*(9), e0238886, doi.org/10.1371/journal.pone.0238886, 2020.

Donato, M.M.: A Statistical Model for Estimating Stream Temperatures in the Salmon and Clearwater River Basins, Central Idaho. US Geological Survey Water Resources Investigations Report 2002-4195, 2002.

Dugdale, S. J., Hannah, D. M., and Malcolm, I. A.: River temperature modelling: a review of process-based approaches and future directions. Earth Sci. Rev. 175, 97–113. doi: 10.1016/j.earscirev.2017.10.009, 2017.

Erickson, T. R., Stefan, H. G.: Linear air/water temperature correlation for streams during open water periods. Journal of Hydrologic Engineering. 5(3): 317-321, doi.org/10.1061/(ASCE)1084-0699(2000)5:3(317), 2000.

Faulkner B.R., Brooks J.R., Keenan D.M., and Forshay K.J.: Temperature Decrease along Hyporheic Pathlines in a Large River Riparian Zone. Ecohydrology. 1;13(1):1-10. doi: 10.1002/eco.2160. PMID: 32983317; PMCID: PMC7513865, 2020.

Ficklin, D. L., Barnhart, B. L., Knouft, J. H., Stewart, I. T., Maurer, E. P., Letsinger, S. L. and Whittaker, G. W.: Climate change and stream temperature projections in the Columbia River basin: habitat implications of spatial variation in hydrologic drivers. Hydrol. Earth Syst. Sci., 18, 4897–4912, https://doi.org/10.5194/hess-18-4897-2014, 2014.

Fischer, H.B., List, E.J., Koh, R.C.Y., Imberger, J., and Brooks, N.H.: Mixing in inland and coastal waters. New York: Academic, 1979.

Gregory, S., Ashkenas, L., Oetter, D., Minear, P., and Wildman, K.: Historical Willamette River Channel Change. In: Willamette River Basin Planning Atlas (D. Hulse, S. Gregory and J. Baker, Eds.), pp. 18-25. Oregon State University Press, Corvallis, 2002a.

Gregory, S., Ashkenas, L., Oetter, D. Wildman, R,, Minear, P., Jett, S., and Wildman, K.: Revetments, In: Willamette River Basin Planning Atlas (D. Hulse, S. Gregory and J. Baker, Eds.), pp. 32–33. Oregon State University Press, Corvallis, 2002b.

https://doi.org/10.5194/egusphere-2022-793
Preprint. Discussion started: 7 September 2022
© Author(s) 2022. CC BY 4.0 License.

Gregory, S., Ashkenas L., Jett, S., and Wildman, R.: Flood inundations/FEMA floodplains. In: Willamette River Basin Planning Atlas (D. Hulse, S. Gregory and J. Baker, Eds.), pp. 28–29. Oregon State University Press, Corvallis, 2002c.

Gregory, S., Ashkenas L., Oetter,D., Minear, P., Wildman, K., Christy, J., Kolar, S., and Alverson, E.: Presettlement Vegetation ca. 1851. In: Willamette River Basin Planning Atlas (D. Hulse, S. Gregory and J. Baker, Eds.), pp. 38–39. Oregon State University Press, Corvallis, 2002d.

Gregory, S., Ashkenas, L., Haggerty, P., Oetter, D. Wildman, K,, Hulse, D., Branscomb, A. and Van Sickle, J.: Riparian vegetation, In: Willamette River Basin Planning Atlas (D. Hulse, S. Gregory and J. Baker, Eds.), pp. 40–43. Oregon State University Press, Corvallis, 2002e.

Gregory, S.V., Frederick J. Swanson, W. Arthur McKee, Kenneth W. Cummins, An Ecosystem Perspective of Riparian Zones: Focus on links between land and water, BioScience, Volume 41, Issue 8, Pages 540–551, https://doi.org/10.2307/1311607, 1991.

Gregory, S., Wildman, R., Hulse, D., Ashkenas, L. and Boyer, K.: Historical changes in hydrology, geomorphology, and floodplain vegetation of the Willamette River, Oregon. River Research and Applications, 35(8), pp.1279-1290, 2019.

Helaire, L.T., Talke, S.A., Jay, D. A. and Mahedy, D.: Historical changes in Lower Columbia River and Estuary Floods and Tides. Journal of Geophysical Research, 124(11) https://doi.org/10.1029/2019JC015055, 2019.

Hudson, A.S., Talke, S.A., and Jay, D.A.: Using satellite observations to characterize the response of estuary turbidity maxima to external forcing. *Estuaries and Coasts* 39(5) DOI 10.1007/s12237-016-0164-3, 2017

Hurst, T. P.: Causes and consequences of winter mortality in fishes. Journal of Fish Biology, 71(2), 315-345, doi.org/10.1111/j.1095-8649.2007.01596.x, 2007.

Jay, D.A., and Naik, P.: Distinguishing Human and Anthropogenic Influences on Hydrological Disturbance Processes in the Columbia River, USA. Hydrological Sciences Journal. 56:7, 1186-1209, https://doi.org/10.1080/02626667.2011.604324, 2011.

Jay, D. A., Leffler, K., and Degens, S.: Long-term evolution of Columbia River tides. Journal of waterway, port, coastal, and ocean engineering, 137(4), 182-191, doi.org/10.1061/(ASCE)WW.1943-5460.0000082, 2011.

Johannessen, C.L., Davenport, W.A., Millet, A. and McWilliams, S.: The vegetation of the Willamette valley 1. Annals of the Association of American Geographers, 61(2), pp.286-302, 1971.

Johnson S.L. and Jones J.A.: Stream temperature response to forest harvest and debris flows in western Cascades, Oregon. Canadian Journal of Fisheries and Aquatic Sciences, 57 (Suppl. 2), 30–39, doi.org/10.1139/cjfas-57-S2-30, 2000.

Kaushal, S. S., Likens, G. E., Jaworski, N. A., Pace, M. L., Sides, A. M., Seekell, D., Belt, D.H., Secor, R.L., and Wingate, R. L.: Rising stream and river temperatures in the United States. Frontiers in Ecology and the Environment, 8(9), 461-466, doi.org/10.1890/090037, 2010.

Landers D., Fernald A., Andrus C.: Off-channel Habitats. In: Willamette River Basin Planning Atlas (D. Hulse, S. Gregory and J. Baker, Eds.), pp. 26-27. Oregon State University Press, Corvallis, 2002.

https://doi.org/10.5194/egusphere-2022-793
Preprint. Discussion started: 7 September 2022
© Author(s) 2022. CC BY 4.0 License.

Lee, K.: Stream Velocity and Dispersion Characteristics Determined by Dye-Tracer Studies on Selected Stream Reaches in the Willamette River Basin, Oregon. U.S. Geological Survey Water-Resources Investigations Report 95–4078, 1995.

Mantua, N., Tohver, I., and Hamlet, A.: Climate change impacts on streamflow extremes and summertime stream temperature and their possible consequences for freshwater salmon habitat in Washington State. Climatic Change, 102(1), 187-223, 2010.

Markovic, D., Scharfenberger, U., Schmutz, S., Pletterbauer,F., and Wolter, C.: Variability and alterations of water temperatures across the Elbe and Danube River Basins. Climatic Change 119, 375–389, doi.org/10.1007/s10584-013-0725-4, 2013.

Mayer, T.D.: Controls of summer stream temperature in the Pacific Northwest. Journal of Hydrology, 475, 323-335. https://doi.org/10.1016/j.jhydrol.2012.10.012, 2012.

Monthly Weather Review (MWR): American Meteorological Society, Online ISSN: 1520-0493, Volume 9 to 17, 1881-1889.

Moore, A. M.: Correlation and analysis of water temperature data for Oregon Streams. United States Geological Survey Water-Supply Paper 1818-K, 53 pages, 1967.

Moore, A. M.: Water temperatures in the lower Columbia River. United States Geological Survey, Circular 551, doi.org/10.3133, 1968.

Mote, P.W.: Trends in temperature and precipitation in the Pacific Northwest during the twentieth century. Washington State University, 2003.

Mote, P.W., Parson E. A., Hamlet, A. F. , Keeton, W. S. , Lettenmaier D., Mantua, N, Miles, E. L., Peterson, D. W.,. Peterson, D. L, Slaughter, R., and Snover, A.K.: Preparing for Climatic Change: The Water, Salmon, and Forests of the Pacific Northwest. Climatic Change 61, no. 1-2, 45-88, doi.org/10.1023/A:1026302914358, 2003.

Mote, P. W., and Salathé, E. P.: Future climate in the Pacific Northwest. Climatic change, 102(1), 29-50, doi.org/10.1007/s10584-010-9848-z, 2010.

Mote, P.W., Rupp, D.E., Li, S., Sharp, D.J., Otto, F., Uhe, P.F., Xiao, M., Lettenmaier, D.P., Cullen, H. and Allen, M. R.: Perspectives on the cause of exceptionally low 2015 snowpack in the western United States, Geophysical Research Letters, 43, doi:10.1002/2016GLO69665, 2016.

Mote, P. W., Li, S., Lettenmaier, D. P., Xiao, M., and Engel, R.: Dramatic declines in snowpack in the western US. Npj Climate and Atmospheric Science, doi:10.1038/s41612-018-0012-1, 2018.

Mote, P.W., Abatzoglou, J., Dello, K.D., Hegewisch, K., and Rupp, D.E.: Fourth Oregon Climate Assessment Report. Oregon Climate Change Research Institute. occri.net/ocar4; accessed online February 4, 2019, 2019.

Naik, P. K. and D. A. Jay.: Human and climate impacts on Columbia River hydrology and salmonids. River Research and Applications. 27: 1270-1276, DOI:10.1002/rra.1422, 2011.

National Academies of Sciences, Engineering, and Medicine 2022. An Approach for Assessing U.S. Gulf Coast Ecosystem Restoration: A Gulf Research Program Environmental Monitoring Report. Washington, DC: The National Academies Press. https://doi.org/10.17226/26335

Notch, J.J., McHuron, A.S., Michel, C.J. , Cordoleani, F., Johnson M., Henderson, M.J. and Ammann, A.J.: Outmigration survival of wild Chinook salmon smolts through the Sacramento River during historic drought and high water conditions. *Environ Biol Fish* **103,** 561–576. https://doi.org/10.1007/s10641-020-00952-1, 2020.

https://doi.org/10.5194/egusphere-2022-793
Preprint. Discussion started: 7 September 2022
© Author(s) 2022. CC BY 4.0 License.

Olden J. D. and R. J. Naiman.: Incorporating thermal regimes into environmental flows assessments: modifying dam operations to restore freshwater ecosystem integrity. Freshwater Biology 55: 86–107, doi.org/10.1111/j.1365-2427.2009.02179.x, 2010.

Oregon Department of Environmental Quality (OR-DEQ): Willamette Basin TMDL and WQMP. Chapter 4: Temperature-Mainstem TDML and subbasin Summary. Accessed from https://www.oregon.gov/deq/wq/tmdls/Pages/willamette2006.aspx, accessed 2021-08-21, 2006.

Payne, S. K.: Dams. In: Willamette River Basin Planning Atlas (D. Hulse, S. Gregory and J. Baker, Eds.), pp. 30-31. Oregon State University Press, Corvallis, 2002.

Petersen, J. and Kitchell, J.: Climate regimes and water temperature changes in the Columbia River: Bioenergetic implications for predators of juvenile salmon. Canadian Journal of Fisheries and Aquatic Sciences - CAN J FISHERIES AQUAT SCI. 58. 1831-1841. 10.1139/cjfas-58-9-1831, 2001.

Pohle I., Helliwell, R., Aube, C., Gibbs, S., Spencer, M. and Spezia, L.: Citizen science evidence from the past century shows that Scottish rivers are warming. Sci. Tot. Envr. 10.1016/j.scitotenv.2018.12.325, 2019.

Rounds, S.A.: Thermal effects of dams in the Willamette River basin, Oregon: U.S. Geological Survey Scientific Investigations Report 2010-5153, 64 p, 2010.

Rounds, S.A.: Temperature effects of point sources, riparian shading, and dam operations on the Willamette River, Oregon: U.S. Geological Survey Scientific Investigations Report 2007-5185, 34 p. (Also available at http://pubs.usgs.gov/sir/2007/5185.), 2007.

Sedell, J.R. and Froggatt, J.L.: Importance of streamside forests to large rivers: The isolation of the Willamette River, Oregon, USA, from its floodplain by snagging and streamside forest removal, Internationale Veriningung fur Theoretische and Angewandte Limnologie Verhandlungen (International Association for Theoretical and Applied Limnology) 22, 1828–1834, 1984.

Steel, E. A., and Lange, I. A.: Using wavelet analysis to detect changes in water temperature regimes at multiple scales: Effects of multi-purpose dams in the Willamette River basin. River Research and Applications, 23(4), 351-359, doi.org/10.1002/rra.985, 2007.

Steel, E. A., Tillotson, A., Larsen, D. A., Fullerton, A. H., Denton, K. P., & Beckman, B. R.: Beyond the mean: the role of variability in predicting ecological effects of stream temperature on salmon. Ecosphere, 3(11), 1-11, doi.org/10.1890/ES12-00255.1, 2012.

Scott, M.H.: Statistical Modeling of Historical Daily Water Temperatures in the Lower Columbia River. Masters Thesis, Portland State University, 2020.

Scott, M.H., Talke, S.A., Jay, D.A. and Diefenderfer, H.: Warming of the Columbia River, 1853-2018. Submitted to Water Resources Research, Submission 2022WR033330, 2022.

Talke, S.A., Mahedy, A., Jay, D.A., Lau, P. Hilley, C., and Hudson,A.: Sea level, tidal and river flow trends in the Lower Columbia River Estuary, 1853-present, Journal of Geophysical Research-Oceans. https://doi.org/10.1029/2019JC015656, 2020.

Taylor, J.E.: Making Salmon: An Environmental History of the Northwest Fisheries Crisis. University of Washington Press, 488pp, 1999.

Thilenius, J.F., 1968. The Quercus garryana forests of the Willamette valley, Oregon. Ecology, 49(6), pp.1124-1133.

Thompson, P. R., Widlansky, M. J., Hamlington, B. D., Merrifield, M. A., Marra, J. J., Mitchum, G. T., and Sweet, W.: Rapid increases and extreme months in projections of United

https://doi.org/10.5194/egusphere-2022-793
Preprint. Discussion started: 7 September 2022
© Author(s) 2022. CC BY 4.0 License.

States high-tide flooding. Nature Climate Change, 11(7), 584-590, doi.org/10.1038/s41558-021-01077-8, 2021.

U.S. Census: Statistics of The United States (Including Mortality, Property, &c.,) in 1860; compiled from the original returns and being the final exhibit of the Eighth Census. Department of the Interior, Washington D.C., Government Printing Office, 1866.

USC&GS (US Coast and Geodetic Survey): Surface Water Temperature and Density, Pacific Coast North and South America & Pacific Ocean Islands. U.S. Government Printing Office, Rockville, Maryland, 1967.

USGS (United States Geological Survey): Willamette River Bathymetric Survey -- Willamette River Water Temperature Investigation. Retrieved July 28, 2022. https://or.water.usgs.gov/projs_dir/will_tmdl/main_stem_bth.html, 2003.

Voelkel J. , Hellman D., Sakuma R., and Shandas V.: Assessing Vulnerability to Urban Heat: A Study of Disproportionate Heat Exposure and Access to Refuge by Socio-Demographic Status in Portland, Oregon. International Journal of Environmental Research and Public Health, DOI: 10.3390/ijerph15040640, 2018.

Wagner, R. W, Stacey, M.T., Brown, L.R. and Dettinger. M.: Statistical models of temperature in the Sacramento-San Joaquin delta under climate-change scenarios and ecological implications. Estuaries and Coasts. 34: 544-556, https://doi.org/10.1007/s12237-010-9369-z, 2011.

Wallick, J.R., Grant, G., Lancaster, S., Bolte, J.P. and Denlinger, R.: Patterns and controls on historical channel change in the Willamette River, Oregon USA. Large Rivers: Geomorphology and Management, Second Edition, pp.737-775, 2022.

Webb B.W. and Walling D.E.: Temporal variability in the impact of river regulation on thermal regime and some biological implications. Freshwater Biology, 29, 167–182, doi.org/10.1111/j.1365-2427.1993.tb00752.x 1993.

Webb, B. W., Clack, P.D., and Walling, D.E.: Water-air temperature relationships in a Devon river system and the role of flow. Hydrological Processes. 17: 3069-3084, https://doi.org/10.1002/hyp.1280, 2003.

Webb, B. W. and Nobilis, F.: Long-term changes in river temperature and the influence of climatic and hydrological factors. Hydrological Sciences Journal. 52(1): 74-85, doi.org/10.1623/hysj.52.1.74, 2007.

Weber, C., Nilsson, C., Lind, L., Alfredsen, K. T., and Polvi, L. E.: Winter disturbances and riverine fish in temperate and cold regions. BioScience, 63(3), 199-210, doi.org/10.1525/bio.2013.63.3.8, 2013.

White, S.M., Justice, C. Kelsey, D.A. ,McCullough, D.A. and Smith, T.: Legacies of stream channel modification revealed using General land Office surveys, with implications for water temperature and aquatic life. Elementals: Science of the Anthropocene 5(3). https://doi.org/10.1525/elementa.192, 2017.

Willingham, W.F.: Army Engineers and the Development of Oregon. United States Army Corps of Engineers, Portland, 259 pp, 1983.

Zhu, S, Nyarko, E.K., and Hadzima-Nyarko, M.: Modelling daily water temperature from air temperature for the Missouri River. PeerJ. 2018 Jun 7;6:e4894. doi: 10.7717/peerj.4894, 2018.